

AD-A240 646



2

Annual Progress Report*

for

"A Compact Laser Photocathode Driven Accelerator for the
Plasma Wake Field Accelerator Program at UCLA"



Funded by SDIO/IST through ONR

Grant No. N00014-90-J-1952

Period of Performance:

June 1, 1990 to May 31, 1991

* This progress report comprises a number of progress reports written by the investigators throughout the year and were sent to the contract monitor on a periodic basis.

This document has been approved
for public release and sale; its
distribution is unlimited.

9 1 9 20 030

91-11229



EXPERIMENTAL, THEORETICAL & COMPUTATIONAL STUDIES OF THE PLASMA WAKE FIELD ACCELERATOR

ONR Grant No. N00014-90J-1952

PROGRESS REPORT NO. 8

June 11, 1991

Preliminary Measurements of a Plasma Produced by a Tubular Lanthanum-Hexaboride Cathode

As mentioned in Report # 5, the plasma wake field accelerator requires a plasma density of 5×10^{13} to $5 \times 10^{14} \text{ cm}^{-3}$ in order to achieve a significant wake field amplitude ($eE > 10 \text{ MeV/m/nCoul}$). Our earlier attempts with RF produced plasmas and BaO coated cathodes resulted in plasma densities which approached $9 \times 10^{12} \text{ cm}^{-3}$. In this report, we will describe the preliminary measurements of a plasma produced by an indirectly heated Lanthanum Hexaboride cathode. The main advantages of Lanthanum Hexaboride (LaB_6) are that: i) LaB_6 has a high emission current density (20 A/cm^2 at 1700°C); ii) it has a low evaporation rate (almost two order of magnitudes lower than tungsten); and iii) it is immune to accidental exposure to air.

The plasma source is tested in a highly evacuated ($p = 3 \times 10^{-8} \text{ Torr}$) chamber. The cathode which consists of an indirectly heated LaB_6 tube (2.5" long, 5/8" O.D., 3/8" I.D.) is suspended in the middle of the chamber (Figure 1). To reduce the cathode heater power requirements, the cathode and the heater filaments are heat shielded by three layers of .003" tantalum sheets. The anode, a tantalum tube (2" long and 1/2" diameter), is placed at an axial distance of about one inch from the cathode. The cathode heater power is on continuously. Either argon or xenon gas is bled into the chamber via a needle valve, and a steady state background pressure in the range 3 to 80 mTorr is established. A discharge voltage pulse of 50 to 100 V is applied to the anode, which accelerates the thermionically emitted electrons from the cathode toward the anode. The accelerated primary electrons ionize the background gas to create a fairly dense plasma. The discharge voltage is pulsed at a rate of 1 Hz

($t_{on} = 3$ ms, $t_{off} = 1$ sec). Figure 2 shows a typical discharge voltage and a discharge current wave form. Note that the discharge current which can be high as 230 A decreases as a function of time due to the finite capacitance of the discharge capacitor bank ($C = 32$ mF).

The primary electrons emitted from the cathode make a single pass through the gas and are collected by the anode. Consequently, the neutral gas ionization fraction is quite low (2 to 10%). Later, an axial magnetic field will be added to confine the electrons radially. The magnetic field would allow us to extend the axial length of the plasma and also force the electrons to make multiple passes between the cathode and the anode before they are lost to the anode by radial diffusion. Thus, the radial confinement of the electrons in the anode region would increase the efficiency of the ionization.

The plasma is diagnosed locally by a small Langmuir probe (area = 4.5×10^{-2} cm²) which measures plasma density, electron temperature, and plasma potential. As shown in Figure 3, a linear voltage ramp ($\Delta V = 100$ V, $\Delta t = 10$ μ s) is applied to the probe and the collected electron current is monitored. Since the voltage ramp is linear in time, the current wave form represents the I-V characteristics of the probe. From the probe characteristics, the plasma density, electron temperature, and the plasma potential are easily deduced. As expected the highest density is found right in front of the cathode (Figure 4a). Unfortunately, due to the high temperature of the cathode, the measurements are limited to only within 1 cm of the cathode. However, one can safely speculate that the inside the cathode the plasma density must be higher. Furthermore, due to the uniform heating of the cathode (i.e. uniform electron emission), one expects the plasma density to be axially uniform within the cathode.

The electron population consists of an energetic tail emitted by the cathode and a denser Maxwellian distribution (secondary electrons) created by ionization of background gas. The relative densities of tail to secondary electrons is quite high (20%) at low background pressures but decreases substantially at higher pressures. The secondary electron temperature ranges between 4 to 7 eV and decreases as a function of increasing neutral gas density. The plasma potential is always below the anode potential. However, as the anode area is increased, the plasma potential becomes more positive and the discharge current increases. These observations indicate that

there is excess electrons in the plasma, which lowers the rate of electron emission from the cathode due to space charge. We intend to increase the area of the anode in the future tests to remedy this problem.

Plasma density measurements show that at a distance of about 1 cm from the cathode edge the plasma density ranges between 0.5×10^{13} to $7.6 \times 10^{13} \text{ cm}^{-3}$ depending on the temperature of the cathode and the background gas pressure. The plasma density is found to be linearly proportional to the neutral gas density (Figure 4b). Furthermore, one must note that at higher background pressures ($p > 40 \text{ mTorr}$) the plasma becomes collisional (electron-neutral collision mean free path = 1cm). Hence, it is paramount that the ionization efficiency be increased in order to lower the background gas pressure. In the near future, we intend to add a strong axial magnetic field to radially confine the electrons. The radial confinement of the electrons would allow us to increase the axial length of the plasma to about 30 cm, create an axially uniform plasma ($\frac{\Delta n}{n} < 0.1$), and substantially increase the ionization efficiency of the gas.

Accession For	
NTIS CRA&I	<input checked="" type="checkbox"/>
DTIC TAB	<input type="checkbox"/>
Unannounced	<input type="checkbox"/>
Justification	
By <i>par ltr.</i>	
Distribution /	
Availability Codes	
Dist	Availability or Special
A-1	



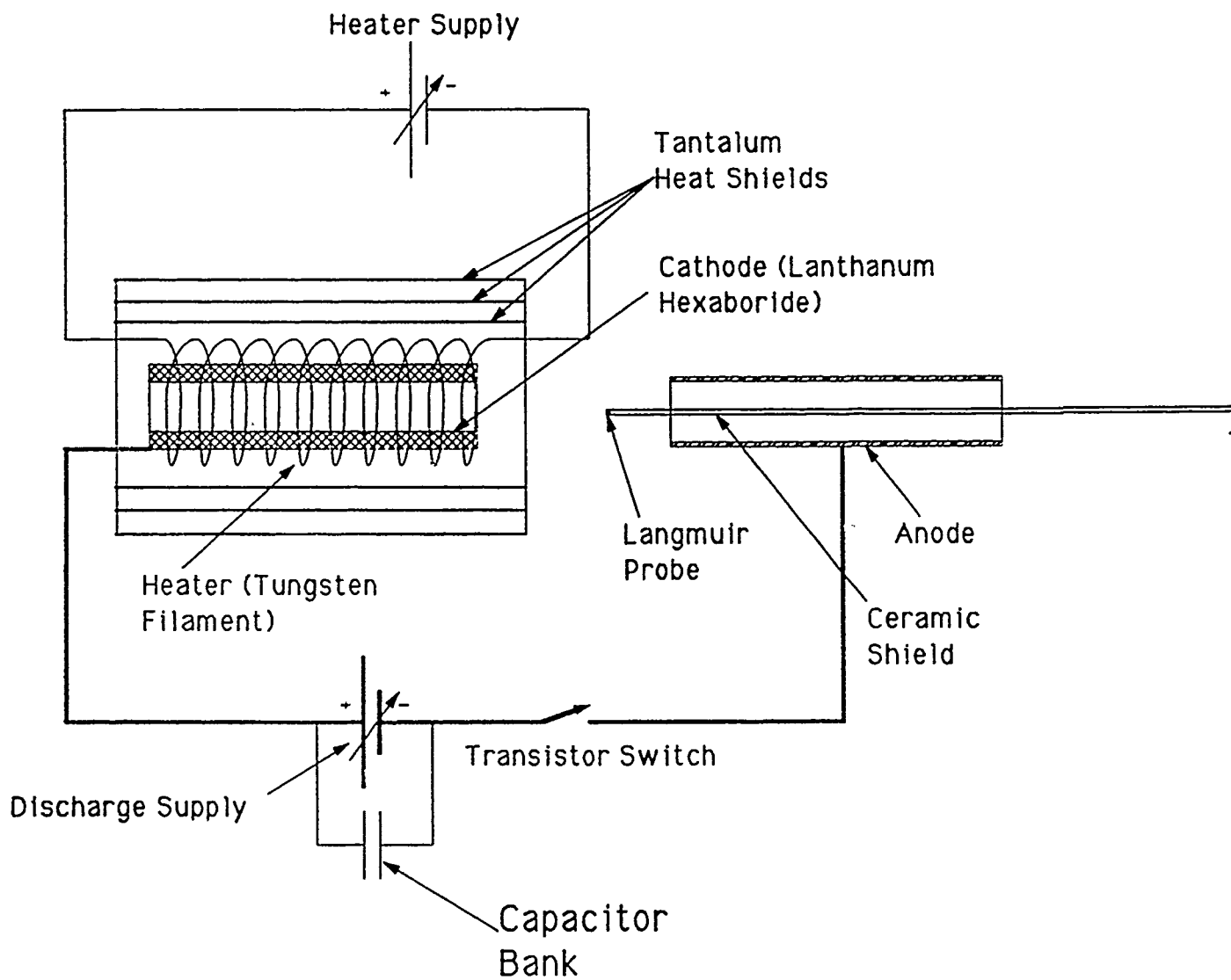
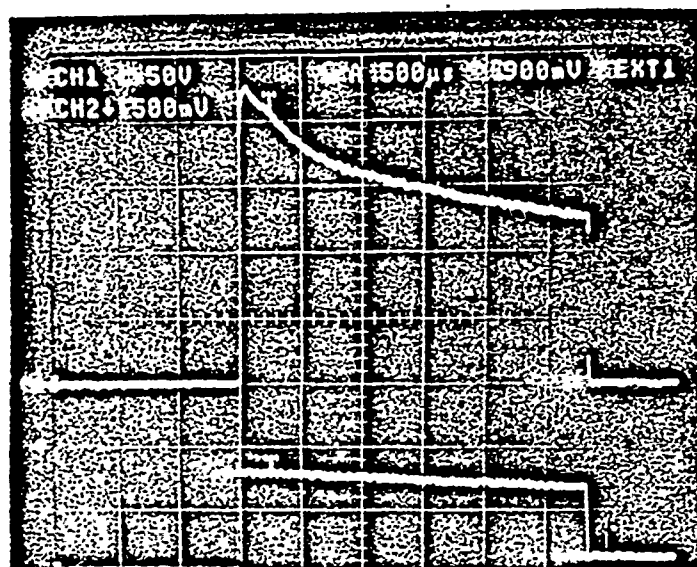


Figure1. Experimental set-up

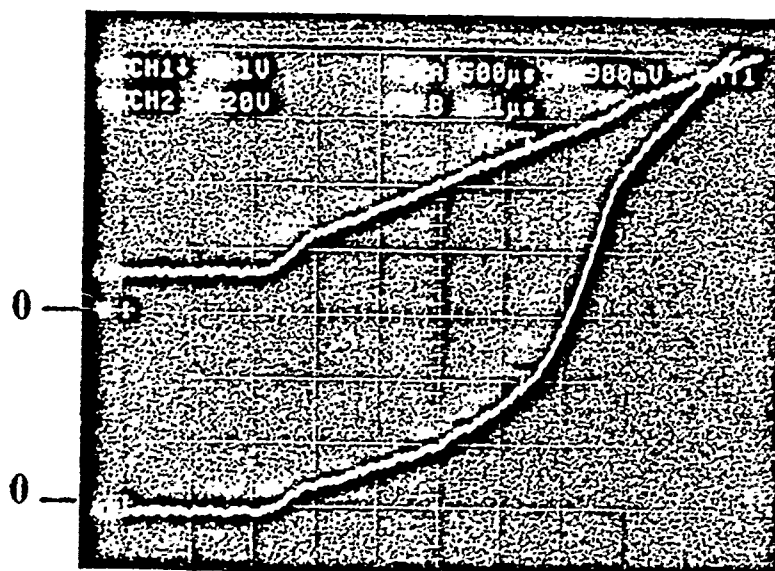


I_{dis} (50 A/div)

V_{dis} (50 V/div)

Time (500 μ s/div)

Figure 2. Discharge voltage and current wave forms



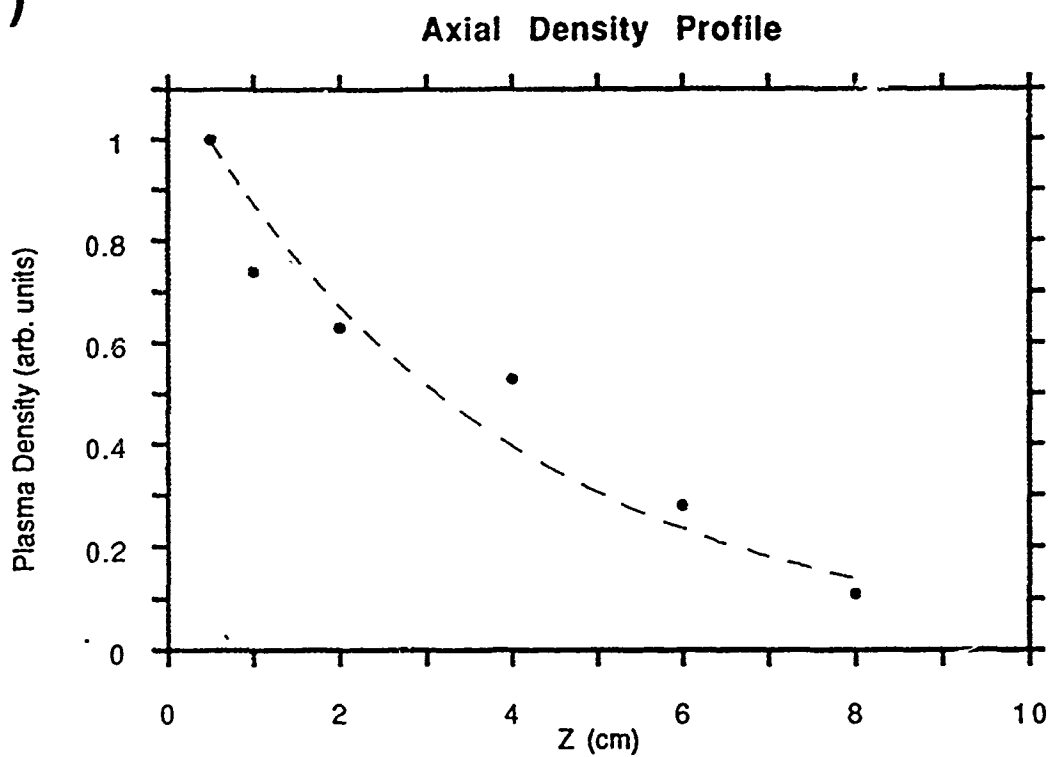
Probe voltage 20 V/div

Probe current .1 A/div

Time (1 μ s/div)

Figure 3. I-V characteristics of the Langmuir probe

a)



b)

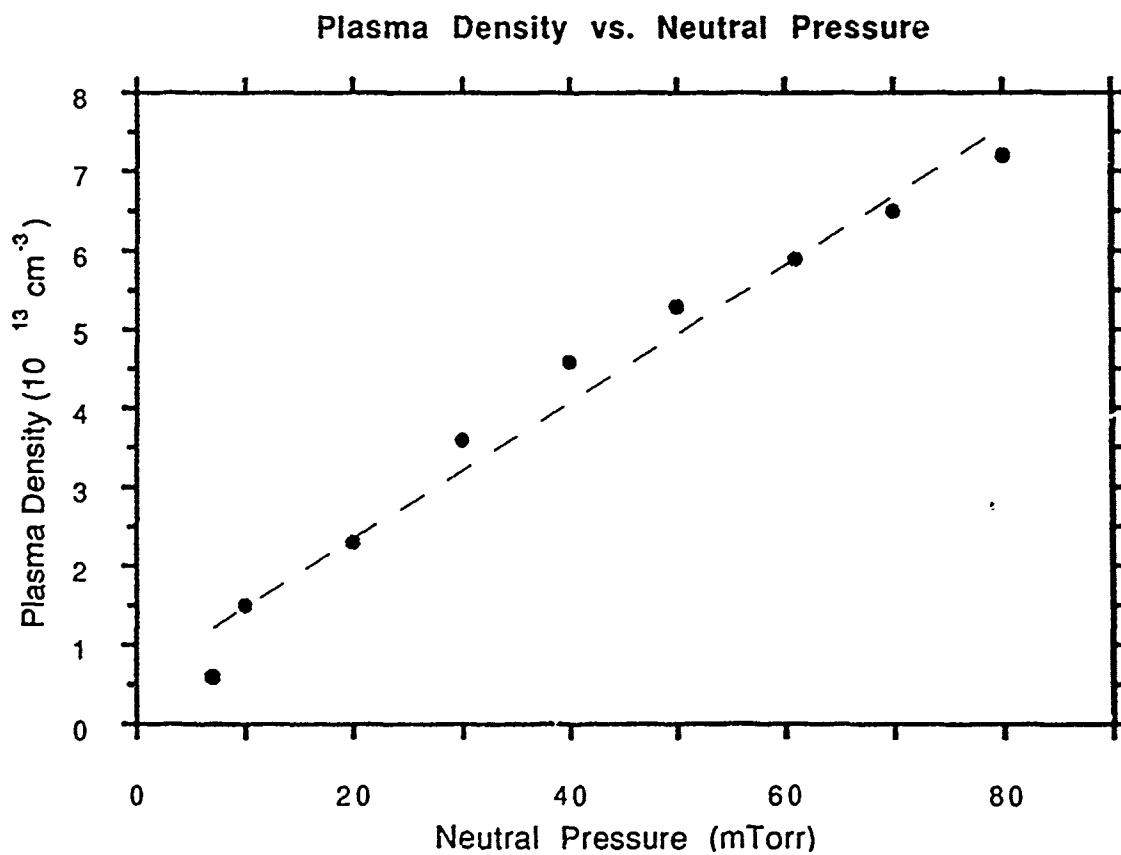


Figure 4

**EXPERIMENTAL, THEORETICAL & COMPUTATIONAL STUDIES
OF THE PLASMA WAKE FIELD ACCELERATOR**

ONR grant no. N00014-90-J-1952.

PROGRESS REPORT NO. 7

April 18, 1991

P.I.: C. Joshi

Microwave Systems for Photocathode Gun and RF Linac at UCLA

Sanghyun Park⁽¹⁾ and David McDermott⁽²⁾

⁽¹⁾Department of Physics

⁽²⁾Department of Electrical Engineering
University of California, Los Angeles, CA 90024

April 18, 1991

Introduction

This note describes the rf systems starting from the locked laser's crystal oscillator to 20 MW of microwave output from the klystron. Details on high power waveguide components[1], modulator[2], and control/diagnostics can be found elsewhere. The main emphasis will be on the frequency multiplier and preamplifier to the klystron. These two systems are to accomplish two objectives:

- (1) Synchronize, or phase lock, the operation of laser and rf systems;
- (2) Provide input signal for klystron with proper frequency and power.

Mixers

Microwave diodes used in mixers are nonlinear devices. Their current-voltage characteristics can be found in any standard textbooks. When this diode is driven by a single frequency sinusoidal wave of sufficient amplitude, the voltage across the diode is clipped, resulting in a rounded square wave. Upon Fourier analysis, this distorted waveform can be shown to contain many waves with frequencies at integral multiples of driving signal frequency. A double balanced mixer has a diode bridge, and produces bipolar square (rounded)

waves at the output.

All mixers have three ports; they are RF (radio frequency), LO (local oscillator), and IF (intermediate frequency). Designation may vary. One conventional application of mixer is to down convert rf wave (demodulation) by feeding LO signal with frequency not so much different from RF. The IF output is at low frequency and it is easier to process. For the purpose of generating harmonics, one port is left open and the other two are used as input and output. Out of six possibilities in choosing which port is used as input and which is left open, one configuration is selected by trial and error for best performance for a particular device. Here the performance means highest output power at the desired harmonic frequency for a given input condition.

Frequency Multiplier

The present frequency multiplier in operation is composed of three stages. The first and the second stages multiply input frequency by five times each and the final stage by three times. Each stage is consisted of one mixer for harmonic generation, one band pass filter to block all unwanted frequency harmonics, and a number of amplifiers to boost power level, to drive the next stage mixer or preamplifier described later. The bandwidths of the filters are narrow enough to block side bands; they are 20, 100, and 300 MHz after the first, second, and final mixer, respectively.

This multiplier is driven by a crystal oscillator at the laser side. The oscillator produces continuous wave at 38.080000 MHz and about 10 mW. Upon multiplication by 75 (which is $5 \times 5 \times 3$), the output signal from the multiplier is at 2.856 GHz of frequency and 100 mW of power, still in steady state.

It must be noted, however, that the output contains side bands. They are 38.08 MHz apart and about 10 dB down from the center frequency. Some efforts have been made to further suppress these 74th and 76th harmonics, without success. Even so, this is not of any concern for the reasons stated later.

Alternative

The description given above applies, in general, to any frequency multiplier utilizing mixer-band pass filter-amplifier combination. One drawback in using mixer is that the conversion efficiency, the ratio of rf power at the desired harmonic frequency to that of input power, diminishes at high harmonics of order greater than, say, 10. If the multiplication factor had been some prime number such as 67 or 79, one would have been compelled to use some other scheme. One example is SRD, or step recovery diode[3]. While the conversion efficiency of mixer is $\sim 1/n^2$, that of SRD is $\sim 1/n$, where n is harmonic number. Instead of nearly square wave output with mixers, this SRD puts out spikes. Although precisely reproducible, its shape is quite irregular and contains rich inventory of harmonics. Some high power devices can put out up to hundreds of watts of power at microwave frequencies.

This has some shortcomings as well. For a good spectral purity, the diode is physically placed inside a resonance cavity. The Q of the cavity must be high and tuning must be done precisely. Great care should be exercised in designing and fabrication of output coupling, too. Despite these technical difficulties, SRD remains to be a strong candidate, depending upon application requirements.

Preamplifier

The klystron, which is the last stage of high power rf system, needs a few hundred watts of input power to produce up to 24 MW for about 2.5 μ S. The preamplifier providing this level of power has been custom made by Pro-Comm. It consists of one solid state amplifier, with output of up to 5 watts, and three stages of triode amplifiers. The maximum output power is 1.3 kW, continuously adjustable down to 20 watts by one variable resistor, which controls electron current in those triodes. The duration of the output power is variable between 1 to 20 μ S and it is determined by an external TTL pulse. The duty cycle must be 0.002 or lower due to limitations of the vacuum tubes.

This amplifier has a very narrow band of gain. It has been tuned to operate at the frequency of (2.856 ± 0.001) GHz, where overall gain of this unit is about 53 dB. At the frequency of the side bands mentioned earlier, the gain

drops by 30 dB. Since the side bands have already 10 dB lower power at the input stage, the output power of these side bands to the klystron will be about 40 dB down from the center frequency, which means that 99.99% of the rf power to the klystron is carried by the wave at the center frequency of 2.856 GHz.

High power capability of this unit may turn out very useful in reducing the laser pulse duration by using the active pulse compression technique[4]. This technique involves using the rf to induce frequency chirp on the laser pulse by co-propagating the two in a nonlinear medium such as lithium niobate (LiNbO_3) crystal. The klystron takes about one quarter of 1.3 kW of full power and the rest may be used for that purpose. This amplifier also has phase jitter of less than ± 1 degree.

Work to be done

The quality of high power rf to the gun and accelerator is dictated by the operation of modulator. Here the quality means phase and amplitude stability of the wave. Since no two capacitors or inductors of the pulse forming network (PFN) are identical, each individual inductors must be tuned precisely in order to minimize ripple in power and phase jitter.

The klystron is of type XK-5, provided by Stanford Linear Accelerator Center. It has been tested at high power by SLAC prior to its shipment to UCLA. In order to prevent electrical breakdown inside the waveguide, all the passage of microwave must be maintained in high vacuum. Currently, high priority is given to the vacuum situation. Once the pressure of nano-Torr range is achieved, high power test of klystron up to 24 MW will be started using all the subsystems described above.

RF power control after the klystron is another item of importance. There are seven waveguide directional couplers available on site. Also to be installed are two variable power dividers and one phase shifter to control the power ratio and relative rf phase between the gun and linac. Absolute calibration of rf power using thermally isolated water load is also in the plan.

S. Park was partially supported by SDIO/IST grant no. N00014-90-J-1952 administered through ONR.

References

- [1] R. B. Neal, ed., *The Stanford Two-Mile Accelerator*, W. A. Benjamin, New York, 1968.
- [2] J.-C. Terrien, CAA-Tech-Note-4/91, March, 1991.
- [3] R. Hall, *Electron. Design*, p.28, January 18, 1965.
R. J. Chaffin, *Microwave Semiconductor Devices*, Wiley Interscience, New York, 1973.
- [4] C. Joshi, private communication

EXPERIMENTAL, THEORETICAL & COMPUTATIONAL STUDIES OF THE PLASMA WAKE FIELD ACCELERATOR

ONR grant no. N00014-90-J-1952.

PROGRESS REPORT NO. 6

February 26, 1991

P.I.: C. Joshi

I. Laser System

The YAG oscillator and the regenerative preamplifier are now working. We have measured between 5 mJ and 6 mJ of energy at 1 μm per single ~ 70 ps long pulse. Frequency quadrupling crystals are being ordered to obtain ~ 500 μJ of energy at 0.25 μm . In future we shall chirp the oscillator pulse and use a grating set-up to expand the pulse to about 300 ps. After amplification we shall recompress using a grating compressor to about 4 ps. We should be able to get the same amount of energy but in a much shorter pulse in this manner.

II. Progress on Photoinjector

The photoinjector gun is now ready. The solenoid magnets are ready but need power supplies. The modulator/klystron is being tested. Operating procedures for the complete linear accelerator facility have been worked out and sent to radiation safety office for approval. Upon approval we shall begin the assembly of the radiation shielding. Once the shielding is inspected, we can hook-

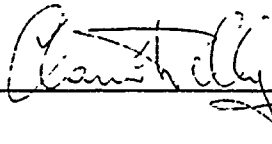
up the power to the gun and make measurements of the dark current. The tentative schedule for this is as follows:

- March 91 Connect gun, laser transport box and connecting tube to the vacuum system and check vacuum.
Bake and get vacuum to $< 10^{-8}$ Torr.
- April 91 Assemble shielding, get inspection from radiation safety, hook-up klystron plumbing. Order magnet supplies.
- May 91 Make dark-current test, measure radiation.
Transport laser to target.
- June 91 Put laser pulses on the photocathode. Make preliminary measurements on the electron beam and emittance.

OPERATING PROCEDURES FOR THE UCLA LINEAR ACCELERATOR FACILITY

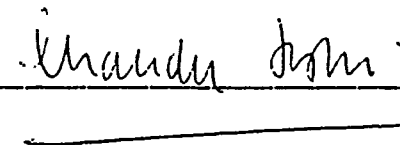
Principle Investigators:

Professor Claudio Pellegrini
Center for Advanced Accelerators
Department of Physics



and

Professor Chan Joshi
Department of Electrical Engineering



February 14, 1991
Version 1.0

1.0 Précis

An RF laser-driven electron gun is being built at UCLA. This electron injector will be used to study the production of high-brightness electron beams, and to drive a high gain, free-electron laser amplifier. Other particle beam physics experiments include plasma wakefield acceleration. All these experiments are performed under the umbrella of the Center for Advanced Accelerators located at the UCLA Linear Accelerator Laboratory.

1.1 Description of the Laboratory

Figure 1 is a diagram of the facility's layout. The facility is located in the northwest corner of the sub-basement in Knudsen Hall. Fig. 1 shows the room containing the YAG laser oscillator, regenerative amplifiers, and pair of frequency doubling crystals. Room B-105 houses the operator's room with extra space available for future expansion. The middle room (B-109) contains two focusing solenoids that straddle the RF electron gun, a laser mirror box, two diagnostic ports, and the Faraday cup at the terminus of the beam line. Lead blocks are shown stacked around the Faraday cup. Surrounding the accelerator is a concrete shield that is a minimum of 12 inches thick.

Figure 2 is an elevation diagram for the middle room of a view facing west. The accelerator components are seen more clearly. The aluminum frame of welded I-beam construction is also visible. This frame provides the means of support for the concrete blocks on the roof of the "bunker." Plywood on the outside of the aluminum frame retains the individual blocks. Plywood or chain-linked fencing retains the blocks on the outer faces of the bunker exposed to lab personnel.

Figure 3 is an elevation diagram for the same middle room of a view facing north. This north facing view shows the access opening in the roof of the bunker near the westernmost wall of the room.

Table 1.0. shows the design parameters for the linear accelerator.

Table 1.0 Design parameters

<i>ELECTRON BEAM</i>	
Energy, nominal	5MeV
Energy spread, r.m.s.	0.2%
Average current	$5 \cdot 10^{-9} \text{A}$
Peak current	160A
Klystron frequency	2.865GHz
Pulse repetition rate	5Hz
Macropulse duration	3.5 μ sec
micropulse duration, r.m.s.	$\approx 6 \text{psec}$
Charge per bunch	$\approx 1 \text{nC}$
Normalized emittance, r.m.s.	15mm-mrad

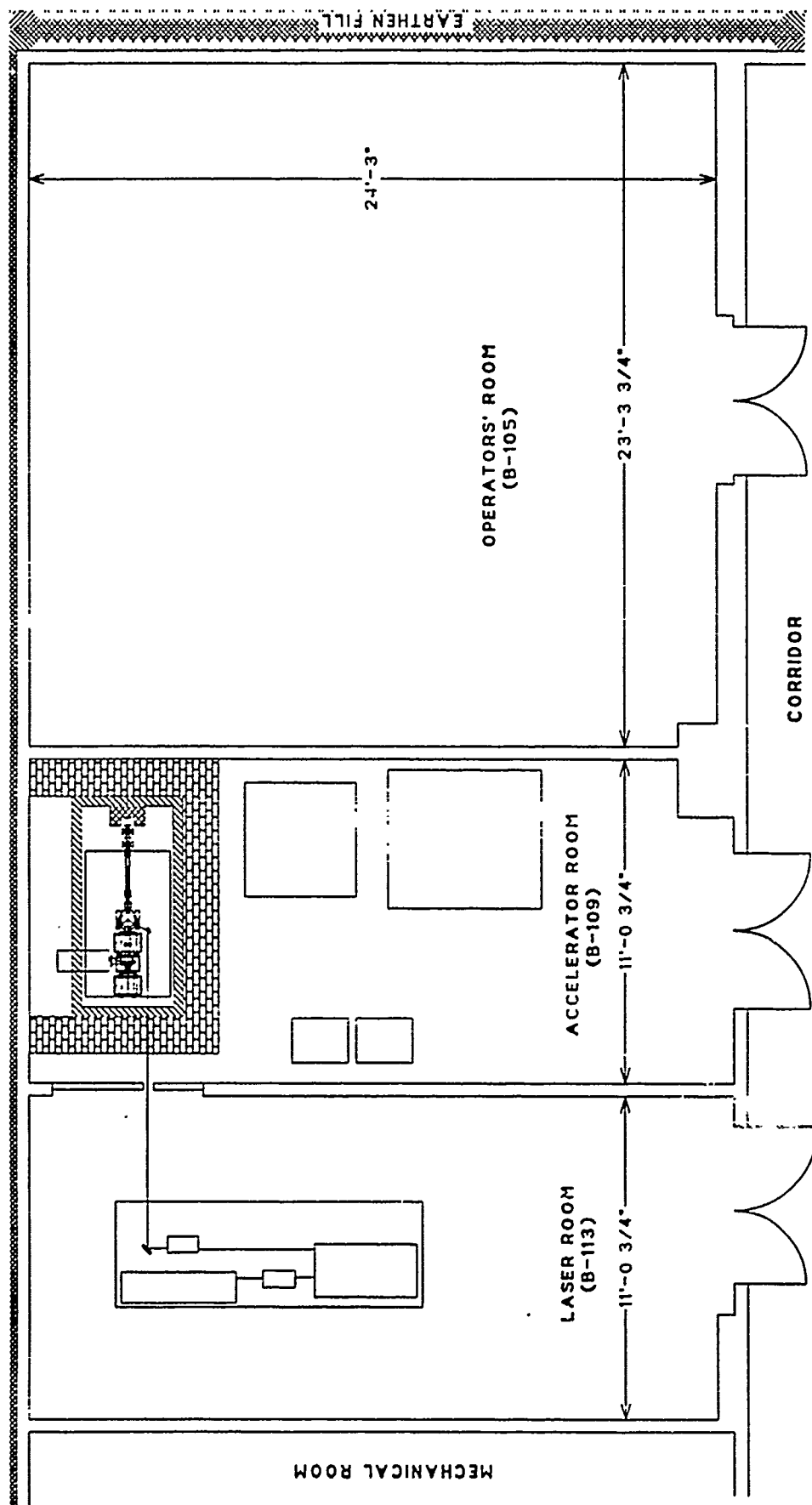


Figure 1 Layout of UCLA's Linear Accelerator Laboratory located in the sub-basement of Knudsen Hall.

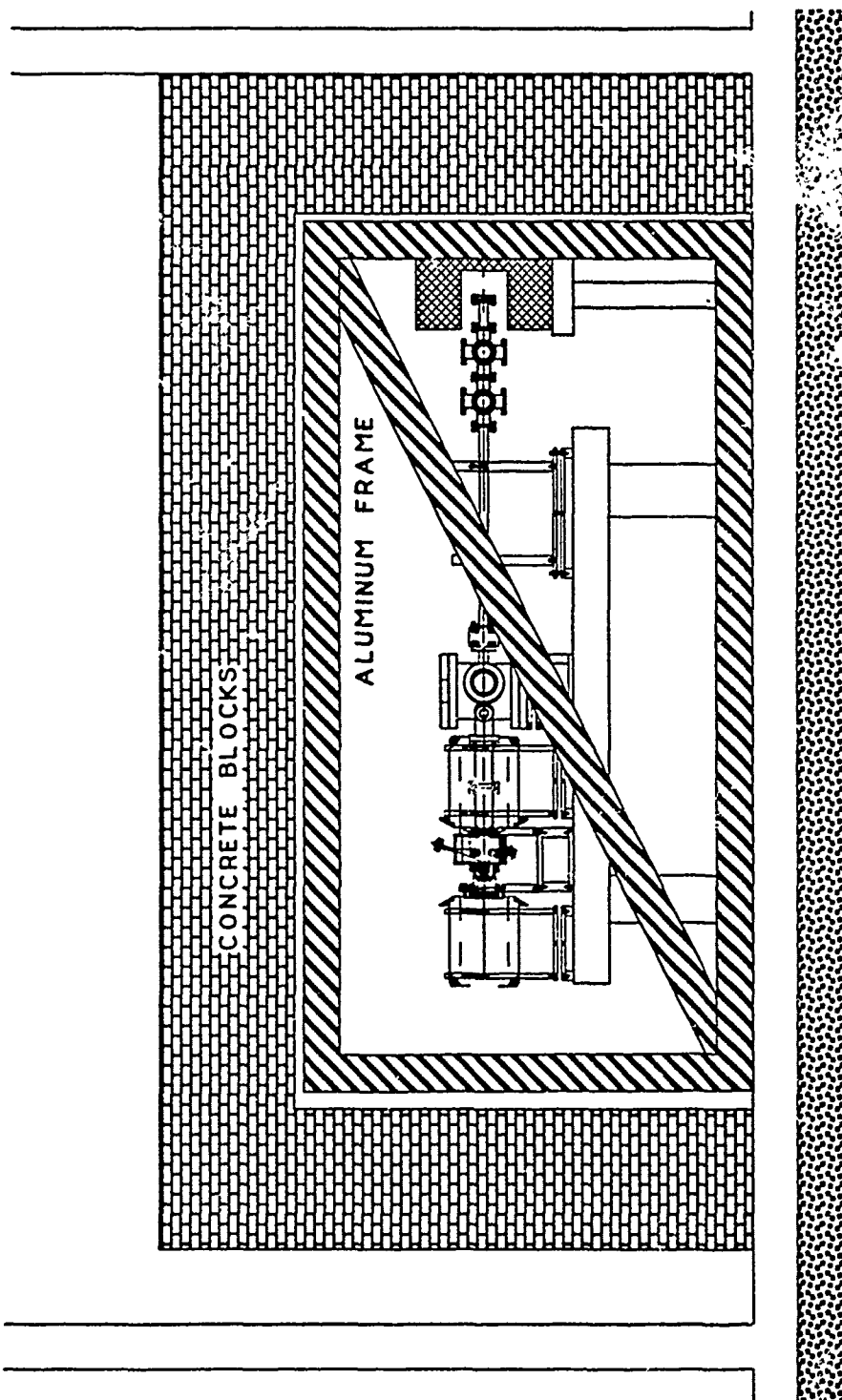


Figure 2 Elevation of accelerator room showing the view facing west.

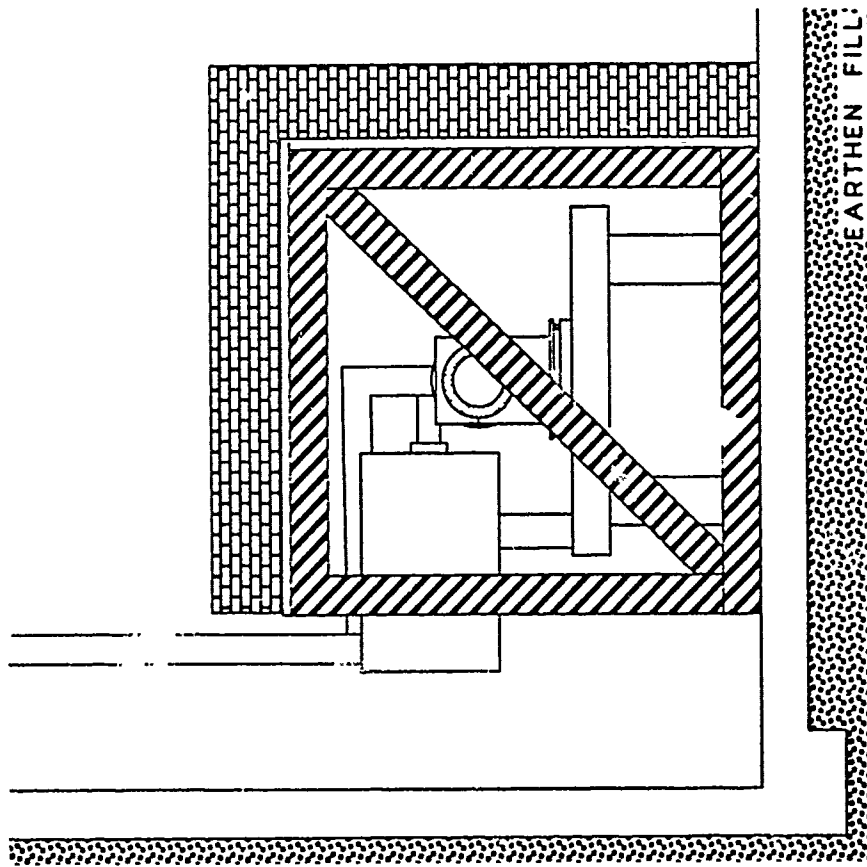


Figure 3 Elevation of accelerator room showing the view facing north. Notice the 2 feet gap in the roof of the concrete bunker.

2.0 Research and Occupational Safety Hazards of the UCLA Linear Accelerator Facility

Potential safety hazards associated with the UCLA infrared free-electron laser are composed of three groups.

1. General laboratory/industrial safety hazards
2. Electrical safety hazards
3. Ionizing radiation safety hazards.

Each group of hazards and their means of control is discussed below.

2.1 General Laboratory/Industrial Safety Hazards

Ordinary industrial hazards involved with the UCLA linear accelerator system (hereafter called the "linac laboratory") include:

1. implosion from failure of vacuum containment
2. toppling of lifting cranes or hoists
3. exposure to class IV laser radiation
4. fire
5. earthquake.

Standard laboratory design, maintenance, operation, and training of personnel should adequately control these hazards.

Injury from implosion is minimal since the entire vacuum vessel will be enclosed in a concrete bunker (See §2.3.3.). In the rooms exposed to class IV laser radiation safety goggles will be used to prevent eye damage. Personnel will be warned not to place their hand in the path of the ultraviolet, the green, or the infrared beam. Warning placards and indicator lights will act as visible reminders. Fire extinguishers rated for electrical fires will be placed in each room of the linac lab. Smoke detectors will be placed in rooms where a machine operator is not always present. Construction of the concrete block bunker will be consistent with the earthquake code requirements of the building, Knudsen Hall.

2.2 Electrical Safety Hazards

Electrical hazards involved in the linac lab include:

1. accidental high voltage discharge
2. electromagnetic interference (EMI)
3. strong magnetic field exposure.

Training to avoid high-voltage accidents is the best preventative. Often the lethal accident occurs when the worker "discovers" an unexpected location at high-voltage or when repairs are done without thoroughly grounding all conducting surfaces. Personnel will be instructed never to work alone on high-voltage equipment. To remind personnel, signs and flashing light indicators will be installed where appropriate. Shorting sticks attached securely to a direct connection to earth ground will be routinely used to short all high-voltage capacitors (e.g., in the modulator) before any maintenance or inspection is performed.

Switching high-voltage pulses in the modulator as well as the klystron assembly is a possible source of radio frequency interference. Likewise the microwave output of the klystron is a possible source of electromagnetic interference. Disruption of laboratory experiments outside (as well as inside) the linac lab must be minimized. Accordingly a metallic barrier has been fitted tightly around the modulator and klystron. RFI gaskets are used around all joints and doors of the aluminum sides of the modulator box. The transformer under the klystron is encased in its own metal enclosure, and a triaxial cable connects the modulator to the klystron with the outer conductor connected to both the chassis of the modulator as well as the transformer cover. Nowhere along the vacuum filled rectangular waveguide connecting the output of the klystron to the electron gun or to the linac section is microwave radiation able to radiate into the air.

Strong magnetic fields will be present wherever an electron beam needs focusing or steering. Examples are: the large permanent-magnetic around the klystron, the two solenoids straddling the electron gun, and the bending dipoles. Signs will be posted nearby stating that a strong magnetic field source is present. Indicator lights will flash when the units are energized.

2.3 Ionizing Radiation Safety Hazards

Interception of the electron beam within the components of the accelerator structure generates high energy x-rays from bremsstrahlung radiation. Two forms of ionizing radiation are produced by these x-rays:

- (1) γ -ray photons
- (2) neutrons.

For γ -rays energies on the order 10 to 15 MeV nuclear capture cross-sections experience a resonance resulting in neutron emission around these energies

and above. A calculation of requirements for shielding gamma-ray and neutron radiation is carried out and presented below.

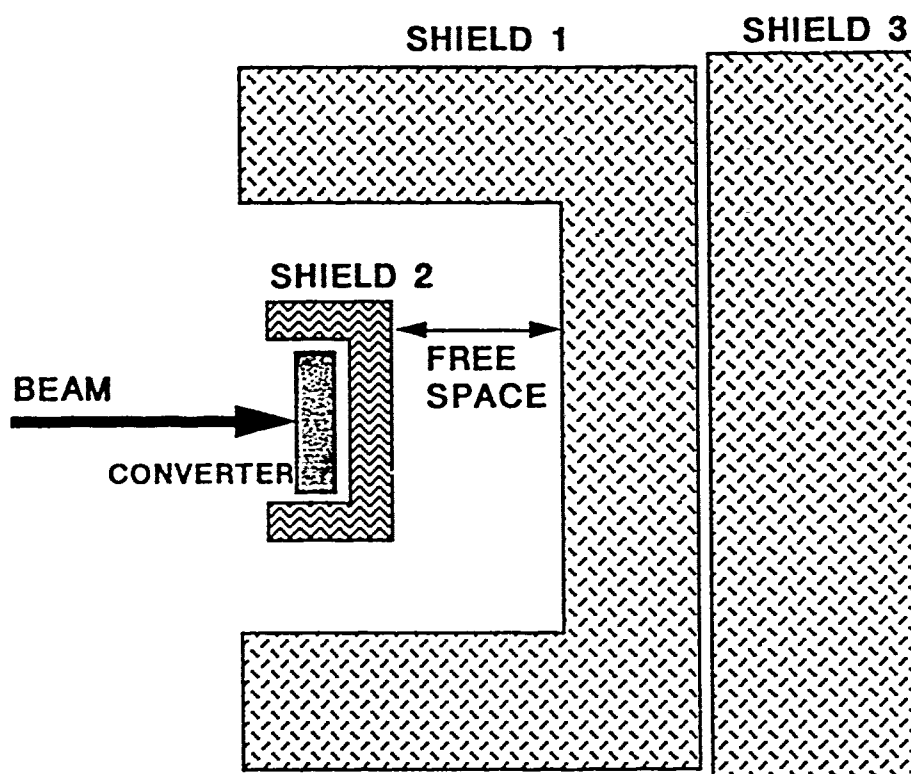
Two modes of operation are to be considered for calculation. First is the mode of routine operation, when the aligned electron beam traverses the entire beam-line unhindered. This is a "high-duty" mode where most of the ionizing radiation is produced at the beam dump. The second mode of interest involves operation of an unaligned electron beam. This "low-duty" mode occurs at turn-on during initial alignment and when an accidental failure causes the e-beam to strike the wall of the vacuum envelope.

The expected average current is so low that activation of accelerator components (including the beam dump) or of the nearby air is considered to be negligible. The possibility of direct exposure to the electron beam is considered to be remote, because even if the beam impinges directly on the metal wall of the beam pipe, the great majority of the charge will be absorbed in the metal wall.

William Barletta has assembled a spread sheet which calculates the dose rates of γ -rays and neutron fluxes given a shielding geometry and the requisite electron beam accelerator parameters. Barletta's spread sheet called "Shield" is based on calculations found in Swenson.¹ As described by Swenson the doses are generally associated with the power in the e-beam, i.e., $\text{dose} \propto E_{\text{beam}} \cdot I_{\text{beam}}$. In particular what is meant by a dose at 0° is $\propto 8.3 \cdot E_{\text{beam}}^2 \cdot I$, whereas for 90° the dose is $\propto 1.4 \cdot E \cdot I$.

The definition of the geometry used for the shielding is diagrammed below. Values for the tenth-value layer of the different shielding material are all taken from Swenson's tabulations. The results for the two operating modes are given next. Asterisks beside an entry indicate an input parameter, all other values are calculated by "Shield."

¹W. Swenson, "Radiological Safety Aspects of the Operation of Electron Linear Accelerators," IAEA, Vienna, 1979.



2.3.1 Routine operation (high duty)

Table 2.1 is indicative of normal operation. The calculations in table 1 are valid for radiation passing through the entire gamut of all three shields. In essence table 1 considers hazards from the beam dump during normal operation.

2.3.2 Turn-on and accidental beam loss (low duty)

Table 2 describes initial operation during commissioning and sudden accidental loss of the e-beam due to failure from steering the beam or from unseen obstructions. Table 2.2 is valid for estimating the radiation reflecting off of shield III and returning back into the room, without benefit of any extra concrete from shield I. The macropulse can be discharged no sooner than every twelve seconds while this 90° x-ray emission is present. This scenario is the worst possible case when having an access gap in the roof of the concrete bunker where preferably no level I shielding needs to be permanently installed. Table 2.2 also depicts estimates of sudden beam loss. When sudden loss of beam is detected and the beam is immediately turned off, even through the gap in the roof little ionizing radiation results. This scenario is what is meant by the "flash hazard."

2.3.3 Summary of ionizing radiation hazard

In summary, control of the ionizing radiation hazard is accomplished using a 1 foot thick (minimum) concrete bunker surrounding the complete e-beam line. Table 2.0 gives a summary of the dose potential for each scenario. During e-beam turn-on and commissioning, the accelerator will be pulsed no more frequently than every twelve seconds in order to avoid the gamma rays emitted at 90° while the beam is intercepted anywhere along the vacuum pipe. Table 2.2 says the gamma ray hazard at 0° is not applicable during turn-on. The gamma ray dose is less for a 0.083Hz repetition rate than for the 5Hz rate of routine operation. In other words the applicable calculation in table 2.2 is for the 90° case. If a bend in the transport system were present then further calculations are required, but no bends are used in this design. Therefore, a 90° calculation is sufficient during turn-on for this straight line design.

Table 2.0 Dose summary

REP RATE (Hz)	DESCRIPTION	GAMMA RAY HAZARD	
		0°	90°
5	Routine operation	NO	NO
0.083	Commissioning during initial turn-on (1 meter away).	NO	NO (Also, no flash hazard)

Table 2.1. Routine operation showing radiation passing all three shields

Beam parameters		Safety levels	
<i>* Italics denote inputs</i>		<i>* Max. <level> (rad/yr)</i>	0.5
<i>* Energy (GeV)</i>	5.0e-03	<i>* Max. single pulse (Rad)</i>	0.20
Gamma	10	<i>* Occupancy factor</i>	1
<i>* Peak current (kA)</i>	0.16	Shielding	
N-part/bunch	6.0E+09	Materials - Pb, Fe, Concrete (Cn), H2O	
Charge/bunch (nC)	1	<i>* Free space (m)</i>	0.5
Pulse energy (J)	0.00	<i>* Shield I</i>	cn
<i>* Pulse length (ps)</i>	6.00	<i>* Thickness I (m)</i>	0.30
Pulse length (mm)	1.8	TVLn - I (cm)	103.0
<i>* n bunches</i>	10	TVLg - I (cm)	48.5
<i>* spacing in wavelengths</i>	35.0	Atten - n - I (dB)	2.91
bunch space ns	12.25	Atten - g - I (dB)	6.18
Macro-pulse (J)	0.0	<i>* Shield II</i>	Pb
Macro-pulse length (ns)	123	<i>* Thickness II (m)</i>	0.120
Current in macropulse (A)	0.007834	TVLn - II (cm)	45.8
<i>* rep rate (Hz)</i>	5	TVLg - II (cm)	4.8
E-beam power (kW)	0.000	Atten - n - II (dB)	2.6
<i>* Duty factor</i>	0.01	Atten - g - II (dB)	24.8
<E-beam power (kW) >	2.4E-06	<i>* Shield III (A-eff) at 0°</i>	21
Accelerator		<i>* Thickness III (m)</i>	1.00
<i>* frequency (GHz)</i>	2.86	<i>* Density - III</i>	2.35
Phase angle (°)	6.17	TVLn - III (cm)	109.8
Energy (MeV)	5	TVLg - III (cm)	64.3
$\Delta E/E (\pm\%)$	0.15	Atten - n - III (dB)	9.11
<i>* No:m Emit (mm-rad)</i>	0.100	Atten - g - III (dB)	15.54
Emittance (m-rad)	1.0E-05	Total attenuation - n 0° (dB)	20.3
Brightness (a/m ² -r ²)	3.2E+09	Total attenuation - g 0° (dB)	52.2
Radiation generation		Total attenuation - n 90° (dB)	4.8
<i>* # of loss points (2m sep.)</i>	1	Total attenuation - g 90° (dB)	30.2
<i>* Convert (C,Al,Cu, Fe, or W)</i>	Cu	DOSE OUTSIDE SHIELD	
Mat. corrector	0.39	Rads per bunch 0°	4.7E-10
Rads per bunch 0°	7.8E-05	Rads per macropulse 0°	4.7E-09
Rads per macropulse 0°	7.8E-04	Flash hazard 0°?	no
Rads per macropulse 90°	2.5E-05	Rads/sec 0°	2.4E-08
Rads/sec 0° @ 1 m	3.9E-03	mRads/hr	0.09
Rad/year 0° @ 1 m	7.8E+02	Rad/year 0°	4.7E-03
Rad/year 90° @ 1 m	2.6E+01	Rad/year 90°	2.5E-02
Neutrons/bunch	0.0E+00	Gamma hazard 0°?	no
Neutrons/sec/cm-2 @ 1m	0.0E+00	Gamma hazard 90°?	no
Neutron dose rate (rem/s)	0.0E+00	Neutrons/bunch	0.0E+00
		Neutron dose rate (rem/yr)	0.0E+00
		Neutron hazard ?	no

Table 2.2. Routine operation with emission at 90° reflected off of shield III.

Beam parameters		Safety levels	
* <i>Italics denote inputs</i>		* <i>M . <level> (rad/yr)</i>	0.5
* <i>Energy (GeV)</i>	5.0e-03	* <i>Max. single pulse (Rad)</i>	0.20
Gamma	10	* <i>Occupancy factor</i>	1
* <i>Peak current (kA)</i>	0.16	Shielding	
N-part/bunch	6.0E+09	Materials - Pb, Fe, Concrete (Cn), H2O	
Charge/bunch (nC)	1	* <i>Free space (m)</i>	1
Pulse energy (J)	0.00	* <i>Shield I</i>	cn
* <i>Pulse length (ps)</i>	6.00	* <i>Thickness I (m)</i>	0.00
Pulse length (mm)	1.8	TVLn - I (cm)	103.0
* <i>n bunches</i>	10	TVLg - I (cm)	48.5
* <i>spacing in wavelengths</i>	35.0	Atten - n - I (dB)	0.00
bunch space ns	12.25	Atten - g - I (dB)	0.00
Macro-pulse (J)	0.0	* <i>Shield II</i>	Pb
Macro-pulse length (ns)	123	* <i>Thickness II (m)</i>	0.000
Current in macropulse (A)	0.007834	TVLn - II (cm)	45.8
* <i>rep rate (Hz)</i>	0.083	TVLg - II (cm)	4.8
E-beam power (kW)	0.000	Atten - n - II (dB)	0.0
* <i>Duty factor</i>	0.01	Atten - g - II (dB)	0.0
<E-beam power (kW) >	4.0E-08	* <i>Shield III (A-eff) at 0°</i>	21
Accelerator		* <i>Thickness III (m)</i>	0.00
* <i>frequency (GHz)</i>	2.86	* <i>Density - III</i>	2.35
Phase angle (°)	6.17	TVLn - III (cm)	109.8
Energy (MeV)	5	TVLg - III (cm)	64.3
$\Delta E/E$ (±%)	0.15	Atten - n - III (dB)	0.00
* <i>Norm Emit (mm-rad)</i>	0.100	Atten - g - III (dB)	0.00
Emittance (m-rad)	1.0E-05	Total attenuation - n 0° (dB)	0.0
Brightness (a/m2-r2)	3.2E+09	Total attenuation - g 0° (dB)	0.0
Radiation generation		Total attenuation - n 90° (dB)	0.0
* <i># of loss points (2m sep.)</i>	1	Total attenuation - g 90° (dB)	0.0
* <i>Convert (C,Al,Cu, Fe, or W)</i>	Cu	DOSE OUTSIDE SHIELD	
Mat. corrector	0.39	Rads per bunch 0°	7.8E-05
Rads per bunch 0°	7.8E-05	Rads per macropulse 0°	7.8E-04
Rads per macropulse 0°	7.8E-04	Flash hazard 0°?	no
Rads per macropulse 90°	2.6E-05	Rads/sec 0°	6.5E-05
Rads/sec 0° @ 1 m	6.5E-05	mRads/hr	233.26
Rad/year 0° @ 1 m	1.3E+01	Rad/year 0°	1.3E+01
Rad/year 90° @ 1 m	4.4E-01	Rad/year 90°	4.4E-01
Neutrons/bunch	0.0E+00	Gamma hazard 0°?	N/A
Neutrons/sec/cm-2 @ 1m	0.0E+00	Gamma hazard 90°?	no
Neutron dose rate (rem/s)	0.0E+00	Neutrons/bunch	0.0E+00
		Neutron dose rate (rem/yr)	0.0E+00
		Neutron hazard ?	no

3.0 Personnel Training

Authorized personnel shall be trained in all the safety aspects of system operation. An assesment of plausible safety hazards was discussed above. A thorough knowledge of the control of these safety hazards by all authorized personnel in the lab is a primary means of their prevention.

Before operating the equipment and before receiving their radiation badges, authorized personnel shall complete the following tasks:

- (1) Complete a Red-Cross approved course in Cardio-Pulmonary Resuscitation (CPR).
- (2) Satisfy all requirements set forth by the UCLA Office of Radiation Safety for radiation workers not dealing with radioactive isotopes.

4.0 System Operation

Separate sub-systems will be discussed in turn. First, however, consider the operation of the overall three-room linac lab. As shown in the first figure, the linac lab consists of three rooms. Room B-105 is reserved for future expansion. Room B-109 contains the RF electron gun assembly and the RF power source. Room B-113 contains the solid-state laser used to activate the photocathode of the RF gun. During normal operation, personnel will primarily occupy room B-105. The fail-safe of last resort is a red "panic button" located near the door in each of the three rooms. Any one of the three panic buttons switches off the circuit breaker supplying the 220V feed into all three rooms. The klystron's power supply and modulator are connected to the circuit breaker of the 480V feed. The circuit breaker for the power supply to the rectifier of the klystron's modulator will be connected to these panic buttons.

4.1 Monitoring equipment

Primary monitoring equipment consists of interlocks and a supervisory microcomputer.

4.1.1 Interlocks

Interlocks are of two kinds: active and passive. The only active interlocks used are of the "key access" variety. A separate key is required to turn-on: the solid-state laser oscillator and the solid-state laser amplifier; the power supply for the klystron's modulator; and the door key limiting access into any of the three rooms of the lab to authorized personnel only. The linac laboratory key is off of the building's master.

Passive interlocks are generally a normally closed circuit through a sensor that detects a condition of: over current; over temperature; loss of

coolant flow in an electromagnet, klystron, or thyrotron; loss of vacuum; or sudden overexposure in a radiation monitor.

4.1.2 Supervisory Microcomputer

At a future date all interlocks and monitoring functions will be handled by a supervisory microcomputer. At the present time, a single interlock circuit will connect all sub-components, such that a single failure will trip all sub-systems to turn off.

4.2 Modulator and Klystron

The modulator has a built in interlock for the console of its power supply. See the Hippotronics operator's manual with regard to the safety features of the DC high-voltage power supply.

4.2.1 Operating Procedures for the "Saturnus" Modulator

The operating procedure for the Saturnus modulator was determined by its builder: Jean-Charles Terrien.

(1) Make sure that the klystron filament heater knob is set to zero, while you turn on the klystron's low voltage power supply switch. A red light should light.

The klystron filament meters should be slowly set to 93V and 3.15A. **Keep the current below 3.4A at all times.** This takes about 5 minutes. The core bias meters should read 5V and between 9 and 15A.

(2) Open the valves for the deionized water.

(3) Make sure that the thyatron heater and reservoir control knobs are set to zero and turn on the low voltage switch on the wall of the modulator.

The reservoir should be set to 3.4V and around 13A, the current being kept below 20A. This takes 10 seconds.

The heater should be set to 6.3V and around 65A, the current being kept below 75A. This takes 1 minute.

Wait 25 minutes. Attempting to cut that time short can destroy the klystron!

(4) Turn on the "Main Power" switch of the 50kV DC power supply console. A green light should light.

(5) Turn on the control power switch of the same unit. Another green light should light.

(6) Turn on the trigger amplifier. A red light should light.

(7) Depress the high voltage "on" button of the power supply console. A red light should light.

(8) Raise the voltage to the desired value (not less than 40kV if using the klystron).

(9) Turn on the pulse generator.

If the power supply trips, turn off the pulse generator and repeat from step 6.

4.3 Nd:YAG/Glass Laser

Operator's Manuals are provided by the manufacture for both the Coherent oscillator and for the Continuum regenerative amplifier.

4.4 Focussing and Steering Magnets

The power supplies for the focussing solenoids shall be interlocked.

UCLA RESEARCH AND OCCUPATIONAL SAFETY
RADIATION SAFETY OFFICE
(213) 206-8204

APPLICATION FOR MACHINE USE
PAGE 3

RESPONSIBLE USER: Claudio Pellegrini AUTHORIZATION #

1. DESCRIPTION OF FACILITY: PROVIDE THE FOLLOWING INFORMATION FOR EACH MACHINE LOCATION LISTED ON PAGE 1 OF THE APPLICATION.

A. DESCRIPTION OF ROOM (INCLUDING LOCATION OF MACHINE(S), SHIELDING, INTERLOCKS, ETC.)

See section 1.1 and figure 1 in the attached operating procedures manual.

B. MONITORING EQUIPMENT (TYPE, MAKE, MODEL NO.)

1. All personnel will receive personal dosimeters.
2. Start-up monitoring will be performed by the radiation safety officer using X-ray monitors.

C. ACCESS CONTROL (DESCRIBE ACCESS CONTROL PROCEDURE FOR PROJECT PERSONNEL, SERVICE PERSONNEL (JANITORS, ETC.) VISITORS)

1. Access to the three rooms of the linac lab is restricted to trained personnel via a door key that is off-master. Visitors shall be escorted.
2. Keys which activate machine controls, e.g., the high-voltage power supply console to the modulator and laser turn-on keys, shall be secured inside the rooms of the linac lab.

2. OPERATION : A COPY OF THE GENERAL OPERATING PROCEDURE COVERING THE USE OF THE MACHINE(S) MUST BE ATTACHED TO THIS APPLICATION OR HAVE BEEN FILED WITH THE UCLA RADIATION SAFETY OFFICE. THE OPERATING PROCEDURE SHALL CONTAIN STATEMENTS AS TO GENERAL OPERATION, MAINTENANCE OF INTERLOCKS, EMERGENCY PROCEDURES, ETC. THE EFFECTIVE DATE ON DATE OF MOST RECENT REVISION MUST APPEAR ON THE PROCEDURE AS WELL AS THE NAME AND SIGNATURE OF THE RESPONSIBLE USER. (MANUFACTURERS OPERATING AND MAINTENANCE INSTRUCTIONS FOR THE MACHINE(S) NEED NOT BE SUBMITTED BUT SHALL BE AVAILABLE FOR REVIEW BY THE RADIATION OFFICE STAFF.) (SEE INSTRUCTIONS FOR SPECIAL REQUIREMENTS AND/OR LIMITATIONS.)

Version 1.0 of the Operating Procedures manual is attached.

RA/SA - 1/84

UCLA RESEARCH AND OCCUPATIONAL SAFETY
RADIATION SAFETY OFFICE
(213) 206-8204

APPLICATION FOR MACHINE USE

RESPONSIBLE USER: Prof. Claudio Pellegrini

AUTHORIZATION #: _____

DEPT: PHYSICS

OFFICE LOCATION: Knudsen Hall, Room: 6-137

PHONE: (213) 206-1677

LIST PERSONNEL FOR THIS PROJECT ON PAGE 2.

THIS APPLICATION IS FOR THE USE OF THE MACHINES LISTED: (LIST TUBE HEADS ONLY)

TYPE	MANUFAC	MODEL NO.	UCLA INV.	MAX. OPERAT. PARAM.			LOCATION
				KVP*	MA**	OTHER	
OTHE	(custom)	-	-	5,000	U (5×10^{-6})		Knudsen Hall Rooms: B-105, B-109, and B-113

(The machine type is an electron beam, radio frequency, linear accelerator.)

* IF KVCP PLACE "C" NEXT TO VOLTAGE

** IF MAXIMUM CURRENT IS LESS THAN 1 MILLIAMPERE, PLACE "U" NEXT TO MA.

IF MORE THAN FIVE MACHINES USED, PLEASE LIST ON SEPARATE SHEET.

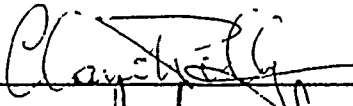
DESCRIPTION OF USE:

 HUMAN USE (REFER TO SPECIAL REQUIREMENTS I RADIATION PROTECTION MANUAL

 CLASS USE: COURSE NO. _____ (DESCRIBE, USING EXTRA SHEET IF NECESSARY)

X OTHER: (DESCRIBE, USING EXTRA SHEET IF NECESSARY) The machine will be used to study the properties of laser-driven high-brightness electron beams and to inject electrons into a free-electron laser amplifier and a plasma wakefield accelerator.

WE CERTIFY THAT THIS PROJECT WILL BE CARRIED OUT IN ACCORDANCE WITH APPLICABLE REQUIREMENTS AND WITHIN THE LIMITS SPECIFIED IN THIS APPLICATION.

RESPONSIBLE USER 

DEPARTMENTAL CONCURRENCE 

RADIATION SAFETY COMMITTEE _____

RADIATION SAFETY OFFICER _____

AUTHORIZATION DATE _____

EXPIRATION DATE _____

UCLA RESEARCH AND OCCUPATIONAL SAFETY
RADIATION SAFETY OFFICE
(213) 825-6018

APPLICATION FOR MACHINE USE
PAGE 2

AUTHORIZATION #: _____

PERSONNEL: (LIST PERSONNEL STARTING WITH RESPONSIBLE USER, LAB SUPERVISOR,
TECHNICAL PERSONNEL)

RADIATION SAFETY OFFICE USE ONLY:

	LAST NAME	FIRST NAME	MI.	SOC. SEC.#	D.O.B.	TR*	FILM
RU***	Pellegrini	Claudio	—	558-94-9657	09MAY35	yes	yes
RU***	Joshi	Chandrasekar	J.	151-52-9261	22JUL53	yes	yes
LS***	Rosenzweig	James Jamie	B.	390-72-8005	01MAY60	yes	yes
	Kolonko	James	J.	399-42-7828	04MAR45	yes	no
	Dodd	James	W.	562-03-5865	30DEC59	yes	yes
	Park	Sanghyun	—	037-44-8619	05OCT47	yes	yes
	Smart	Timothy	M.	501-60-3529	15JUL40	yes	yes
	Hartman	Spencer	C.	558-19-5589	16JAN64	yes	yes
	Robin	David	S.	026-38-8111	20JUL63	yes	no
	Davis	Joseph (Pepe)	G.	549-96-0647	28MAY67	yes	yes
	Hairpetian	Garnick	—	546-49-5020	27DEC59	yes	yes
	Smolin	John	A.	074-44-4881	15SEP67	yes	yes
	Travish	Gil	A.	545-83-9679	30SEP67	yes	no

*TR = TRAINING

* TRAINING: IT IS A CONDITON OF THE APPROVAL OF THIS PROJECT THAT *
* PERSONNEL WORKING WITH RADIOACTIVE ISOTOPES BE TRAINED IN RADIA- *
* TION SAFETY AND ISOTOPE HANDLING PROCEDURES. TRAINING SHALL BE *
* PROVIDED BY THE RESPONSIBLE USER. NEW PERSONNEL SHOULD RECEIVE *
* SUCH TRAINING PROMPTLY. UCLA RADIATION SAFETY OFFICE STAFF WILL *
* PROVIDE ASSISTANCE FOR SUCH TRAINING. *

RA/SA - 1/84

UCLA RESEARCH AND OCCUPATIONAL SAFETY
RADIATION SAFETY OFFICE
(213) 206-8204

APPLICATION FOR MACHINE USE
PAGE 3

RESPONSIBLE USER: Claudio Pellegrini AUTHORIZATION #

1. DESCRIPTION OF FACILITY: PROVIDE THE FOLLOWING INFORMATION FOR EACH MACHINE LOCATION LISTED ON PAGE 1 OF THE APPLICATION.

A. DESCRIPTION OF ROOM (INCLUDING LOCATION OF MACHINE(S), SHIELDING, INTERLOCKS, ETC.)

See section 1.1 and figure 1 in the attached operating procedures manual.

B. MONITORING EQUIPMENT (TYPE, MAKE, MODEL NO.)

1. All personnel will receive personal dosimeters.
2. Start-up monitoring will be performed by the radiation safety officer using X-ray monitors.

C. ACCESS CONTROL (DESCRIBE ACCESS CONTROL PROCEDURE FOR PROJECT PERSONNEL, SERVICE PERSONNEL (JANITORS, ETC.) VISITORS)

1. Access to the three rooms of the linac lab is restricted to trained personnel via a door key that is off-master. Visitors shall be escorted.
2. Keys which activate machine controls, e.g., the high-voltage power supply console to the modulator and laser turn-on keys, shall be secured inside the rooms of the linac lab.

2. OPERATION : A COPY OF THE GENERAL OPERATING PROCEDURE COVERING THE USE OF THE MACHINE(S) MUST BE ATTACHED TO THIS APPLICATION OR HAVE BEEN FILED WITH THE UCLA RADIATION SAFETY OFFICE. THE OPERATING PROCEDURE SHALL CONTAIN STATEMENTS AS TO GENERAL OPERATION, MAINTENANCE OF INTERLOCKS, EMERGENCY PROCEDURES, ETC. THE EFFECTIVE DATE ON DATE OF MOST RECENT REVISION MUST APPEAR ON THE PROCEDURE AS WELL AS THE NAME AND SIGNATURE OF THE RESPONSIBLE USER. (MANUFACTURERS OPERATING AND MAINTENANCE INSTRUCTIONS FOR THE MACHINE(S) NEED NOT BE SUBMITTED BUT SHALL BE AVAILABLE FOR REVIEW BY THE RADIATION OFFICE STAFF.) (SEE INSTRUCTIONS FOR SPECIAL REQUIREMENTS AND/OR LIMITATIONS.)

Version 1.0 of the Operating Procedures manual is attached.

RA/SA - 1/84

EXPERIMENTAL, THEORETICAL & COMPUTATIONAL STUDIES OF THE PLASMA WAKE FIELD ACCELERATOR

PROGRESS REPORT NO. 5

January 8, 1991

Plasma Source

As reported earlier in the Progress Report # 4, the amplitude of the accelerating wake field depends on several parameters including the plasma density, electron beam density and beam size. Figure 1 which is reproduced from the previous report shows the results of a numerical calculation where the amplitude of the accelerating field is plotted as a function of plasma density for different beam densities and beam sizes. It can be seen that for a typical Gaussian electron beam ($Q = 1 - 10$ nC, $\Delta t = 2 - 10$ ps, $\Delta \sigma_r = 30 - 300$ μ m), the required plasma density is between 5×10^{13} to 10^{15} cm^{-3} . Moreover, the plasma should be about a centimeter in diameter, at least 10 cm long, and highly ionized. Two different plasma sources - an RF produced plasma and a pulsed DC discharge plasma - which can satisfy the above conditions are being developed and tested in laboratory.

1. RF Produced Plasma

The RF plasma is generated by a 27 MHz, 650 W power supply. The RF supply is connected to a Nagoya type III copper antenna (Fig. 2a) via a load-matching network. The copper antenna fits snugly around a cylindrical quartz tube (diam. = 2 cm, length = 40 cm), which is evacuated to a base pressure of 5×10^{-5} Torr. Subsequently, Argon gas is bled into the tube ($p = 5 \times 10^{-3}$ Torr) where it is ionized by RF breakdown to create a dense plasma under the antenna. The plasma density is measured by a Langmuir probe, and independently verified by microwave interferometry. The measurements show that the radial plasma potential is roughly Gaussian with a peak density approaching 10^{13} cm^{-3} . Axially, the plasma density is fairly uniform under the antenna and drops off rapidly outside. The neutral density in the tube is about 1.5×10^{14} cm^{-3} ($p = 5 \times 10^{-5}$ Torr), therefore only about 10% of Ar atoms are ionized. It has been observed that the plasma density increases linearly with the RF power (at least in the range between 100 to 650 W). Accordingly, to achieve a density of 10^{14} cm^{-3} , an RF supply of about 5 KW is required. By the end of the January, we expect to start

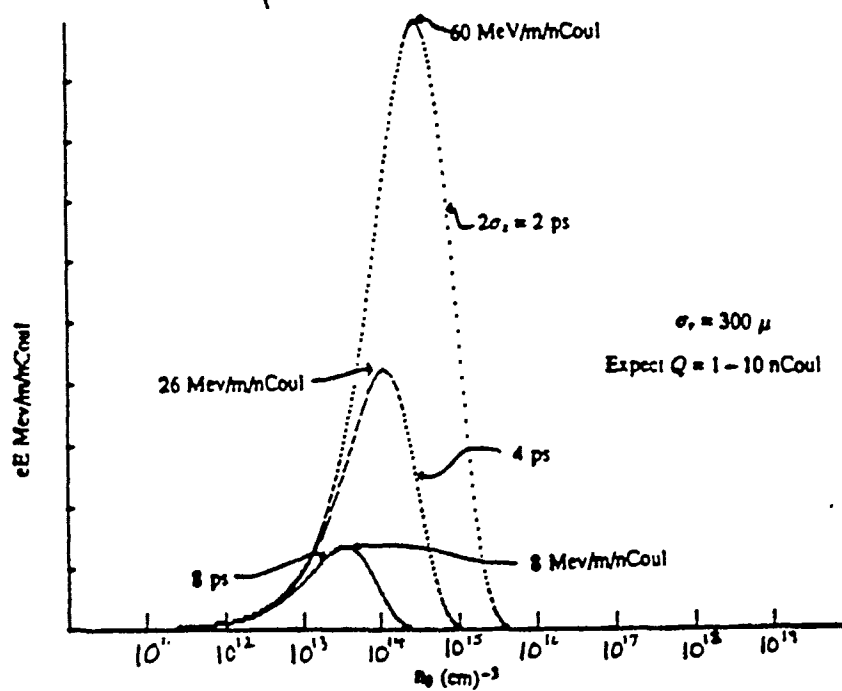
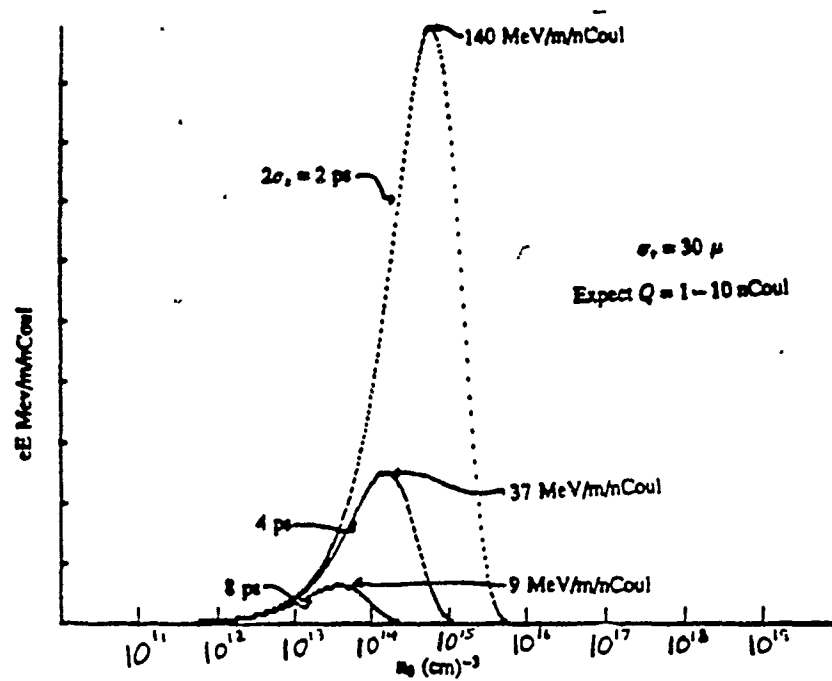
testing a 2.5 KW RF supply which should produce a plasma with a density in the range of high 10^{13} cm^{-3} .

The main advantage of an RF produced plasma is that the plasma is free of any electrodes which could interfere with the electron beam. Secondly, the axial length of the plasma can be easily controlled from outside by adjusting the length of the antenna. However, the main disadvantage is that plasma parameters depend strongly on antenna tuning which can change unpredictably from day to day.

2. Pulsed, DC Discharge Plasma

The second source - a low-voltage, pulsed, DC discharge which is inherently highly quiet and reproducible - is also being simultaneously tested. The limiting factor in achieving a high plasma density in D.C. discharges is the cathode emission current. Consequently, we have used a BaO impregnated tungsten cathode with a very high emission current (10 A/cm^2 compared to less than 2 A/cm^2 for pure tungsten). The cathode (Fig. 3a) has been machined into the shape of a helical filament (diam. = 0.5", length = 1", thickness = 0.040") and is heated to about 1200° C in a highly evacuated chamber ($p = 2 \times 10^{-7} \text{ Torr}$). An anode located at a distance of 5 cm from the cathode is pulsed (pulse width = 1 ms, frequency = 1 Hz) to a positive voltage of + 60 V. In the future, the anode will be hollow in order to accommodate the electron beam. The electrons emitted from the cathode ionize the surrounding Ar gas ($p = 20 \text{ mTorr}$) and are subsequently collected by the anode. The cathode emission current can reach as high as 100 A (Fig. 3b). Due to the fact that the externally imposed axial magnetic field ($B < 50 \text{ G}$) was insufficient to confine the plasma, the plasma density measured near the cathode was only about $7 \times 10^{12} \text{ cm}^{-3}$. In addition, due to ion sputtering, the BaO coating is destroyed very rapidly (about 30 minutes), as a result of which the emission current falls to less than a few miliamps.

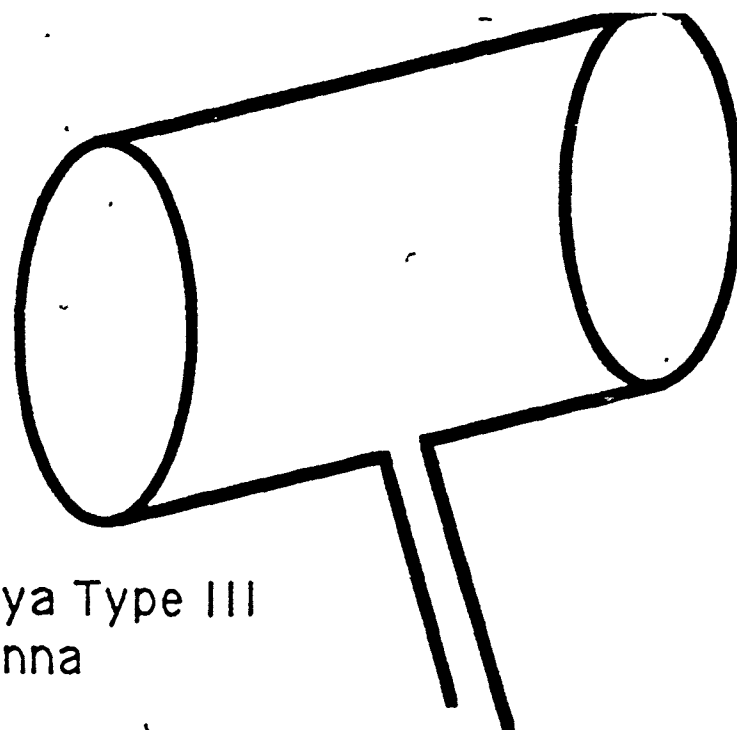
To improve the situation, the cathode will be replaced with an indirectly heated Lanthanum Hexaboride tube (2.5" long, 5/8" O.D., 3/8" I.D.) which has an even higher emission current (20 A/cm^2) and is immune to ion sputtering or poisoning by contamination. Furthermore, Helmholtz coils capable of producing axial fields in the neighborhood of a KG will be employed to confine the plasma radially. With these improvements, we expect to produce a very uniform, high density plasma in the near future.



Wakefield Amplitude vs. Plasma Density (Gaussian Beams)

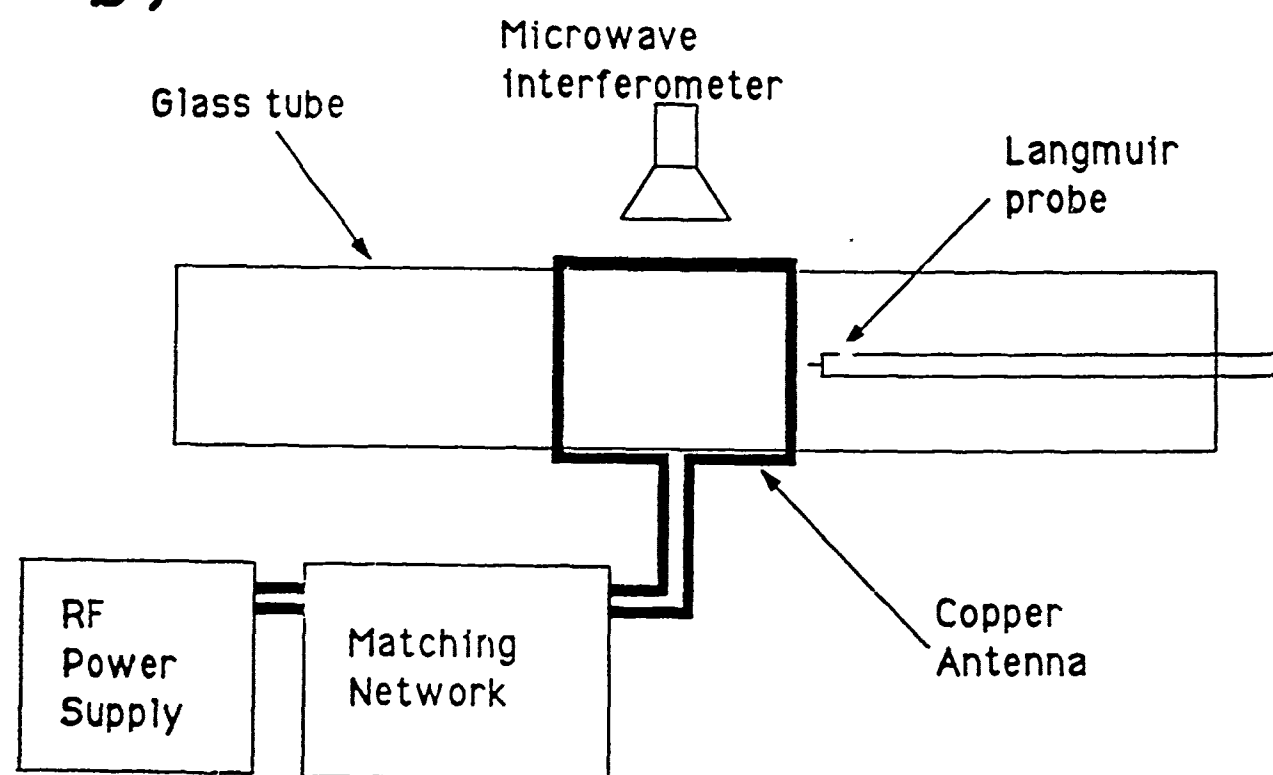
Figure 1

a)



Nagoya Type III
Antenna

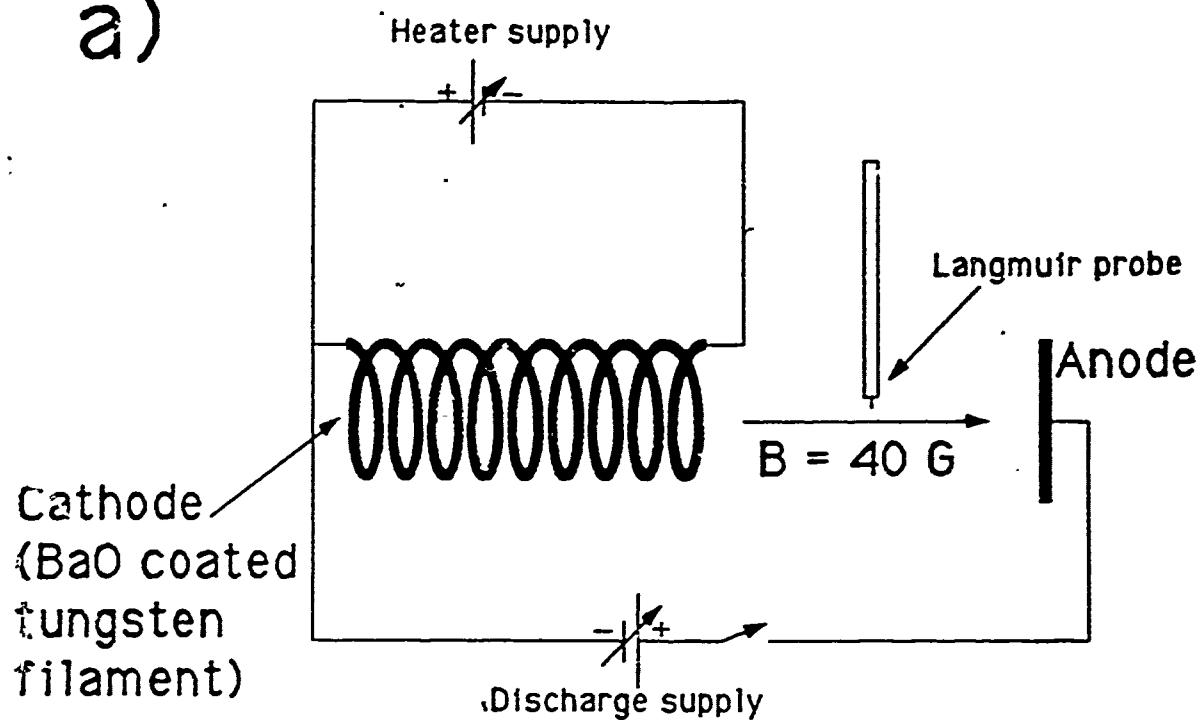
b)



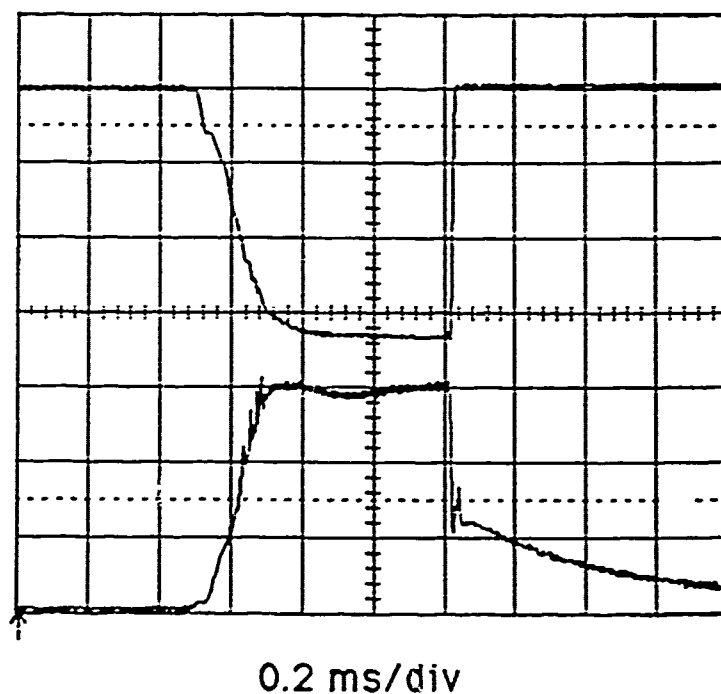
$f \approx 27 \text{ MHz}$
 $P \approx 650 \text{ W}$

Figure 2

a)



b)



discharge current
25 A/div

ion saturation
current 0.5 mA/div

Figure 3

**EXPERIMENTAL, THEORETICAL & COMPUTATIONAL STUDIES
OF THE PLASMA WAKE FIELD ACCELERATOR**

ONR grant no. N00014-90-J-1952.

PROGRESS REPORT NO. 4

December 4, 1990

P.I.: C. Joshi

This report is basically the poster paper presentation by the author and his co-investigators at the annual Division of Plasma Physics meeting in Cincinnati. It reports the current status of this project as of November, 1990.

Design of a Plasma Wakefield Accelerator

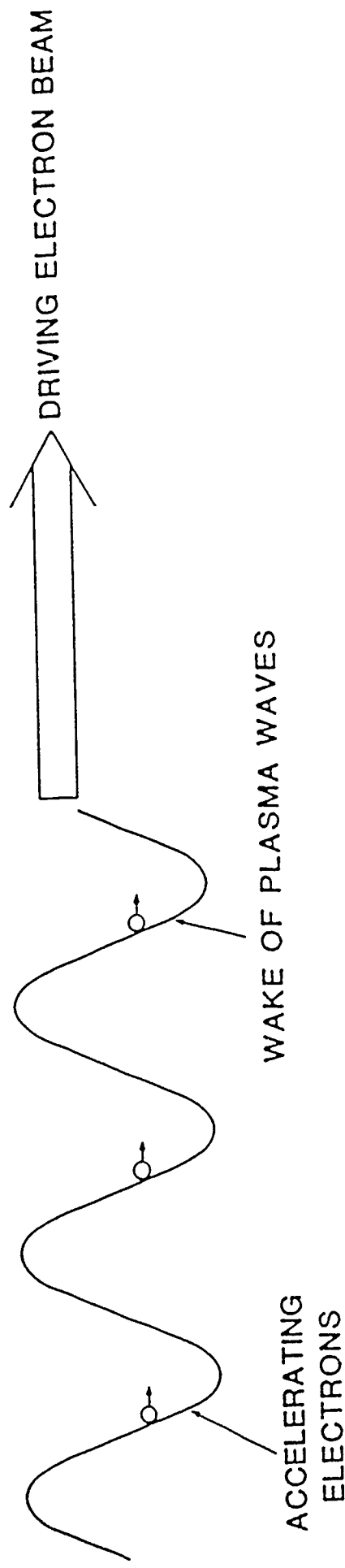
Experiment at UCLA

Supported by SDIO through ONR

J. Smolin, T. Katsouleas, C. Joshi, C. Pellegrini, and P. Davis, **UCLA**

A collaboration has begun at UCLA to build a photocathode-driven, 16-20 MeV RF LINAC which will be used for both Free Electron Laser (FEL) and Plasma Wakefield Accelerator (PWA) experiments. This poster describes the progress and PWA design for the experiments scheduled for mid 1991.

THE PLASMA WAKEFIELD ACCELERATOR



- WAKE EXCITED BY SPACE-CHARGE FORCE OF e^- BEAM
- WAKE PHASE VELOCITY = DRIVING BEAM VELOCITY $\approx c$
(Like a wake tied to a motorboat)
- ELECTRONS INJECTED BEHIND THE DRIVE BEAM "SURF" THE WAKE TO GAIN ENERGY
- MAXIMUM ACCELERATING GRADIENT IN PLASMA DENSITY n_0 IS

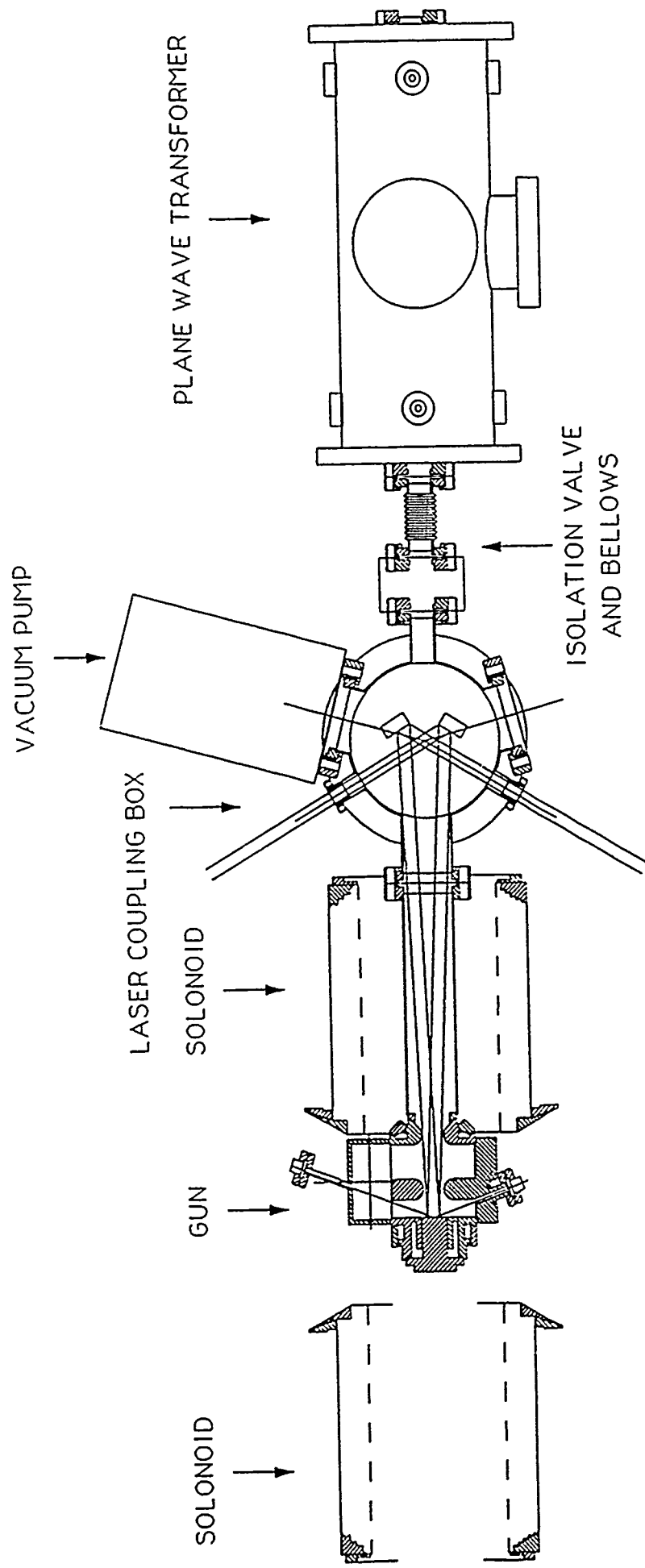
$$eE \sim \sqrt{n_0} \quad eV/cm$$

Idea of the PWA

- A dense bunch of electrons moves through the plasma
- The plasma is disturbed by the bunch, exciting a density wake. This is similar to the wake caused by a boat moving through water.
- The wake contains extremely high electric fields.
- A smaller 'witness' pulse arriving later may then be accelerated by these fields, achieving very high energy in a relatively short distance.

Summary of Beam Characteristics

- Energy: 16 MeV
- Charge: 1-10 nanoCoulombs
- Bunch Length: 2-10 picoseconds
- Longitudinal Pulse Shape: Gaussian (initially)
- Normalized Emittance: 10π mm-mrad
- Witness Pulse: variable delay



THE DETAILS OF THE UCLA PHOTOINJECTOR-DRIVEN ELECTRON LINAC

ELECTRON ACCELERATOR

TRIPOLET

DIPOLE

TO FEL EXPT.

PLASMA WAKE FIELD EXPT.

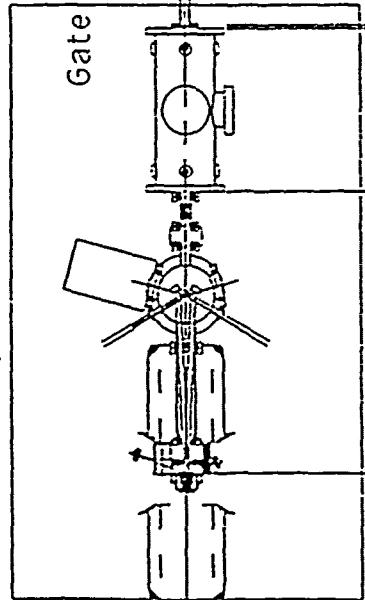
BEAM LINE

Beam Diagnostics

Gate Valve

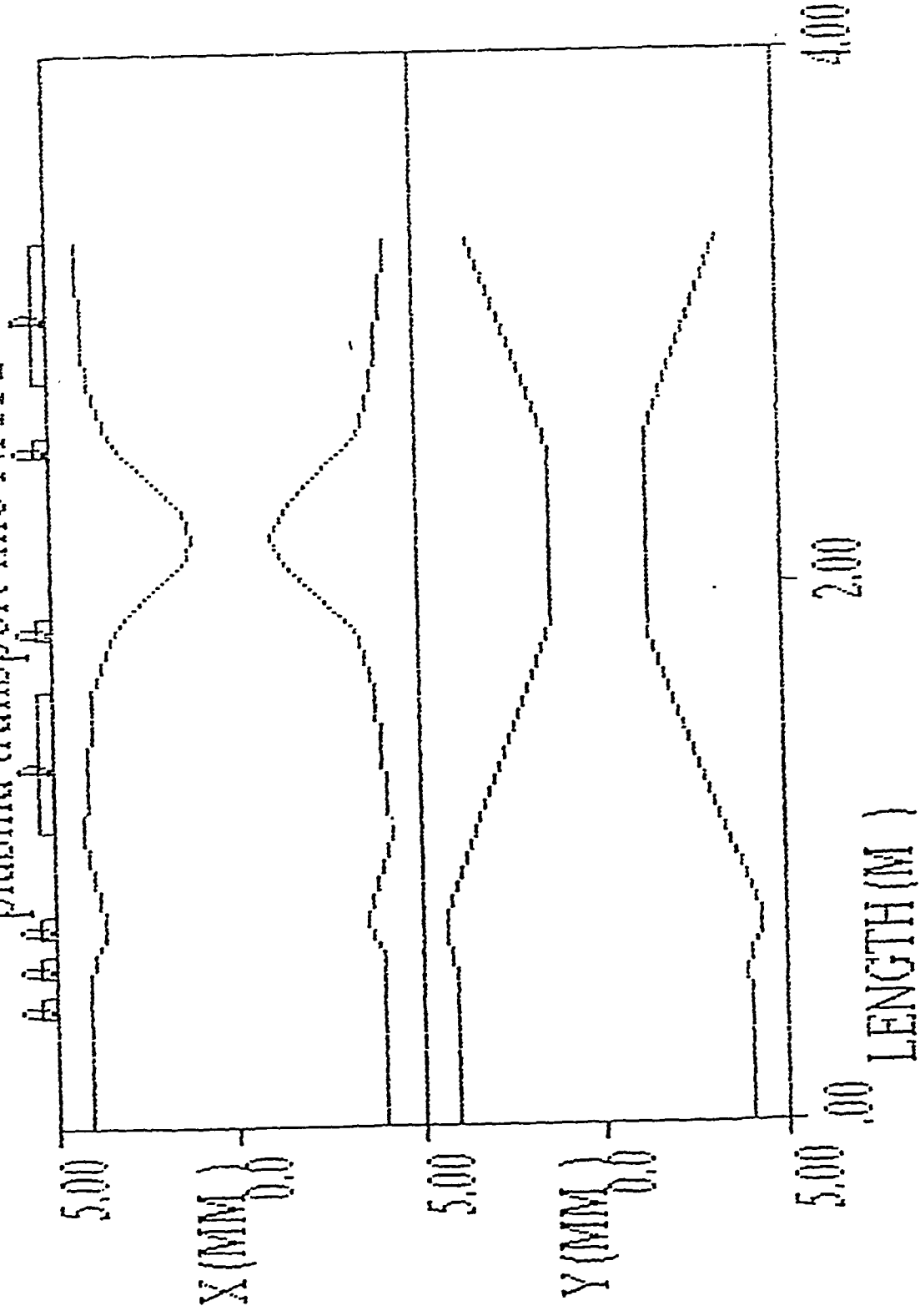
Pumping Port

TO PLASMA EXPT.



ELECTRON ACCELERATOR AND THE
BEAM LINE

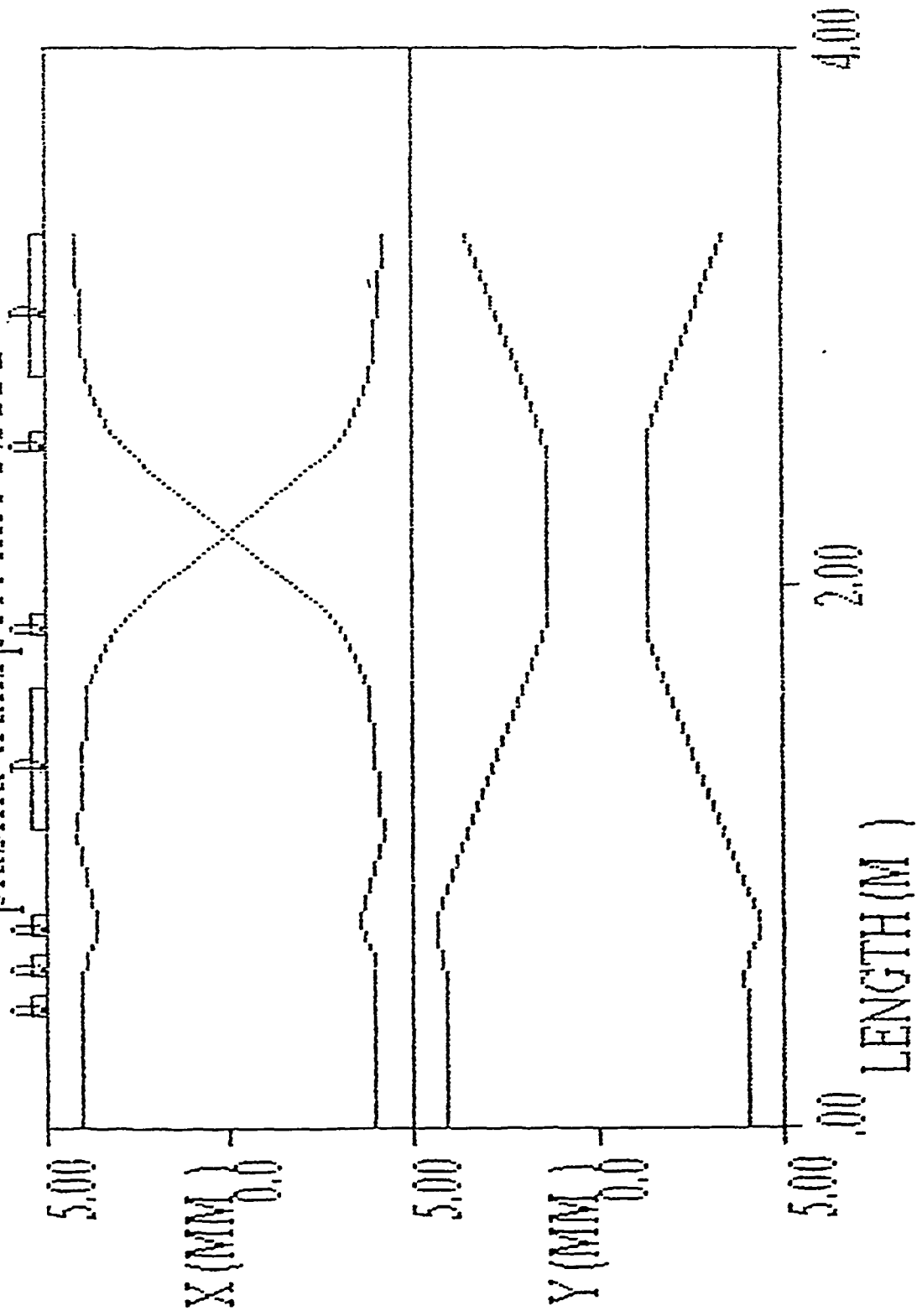
plasma transport line NAT1



TRANSPORT Simulation of Beam Line to Plasma

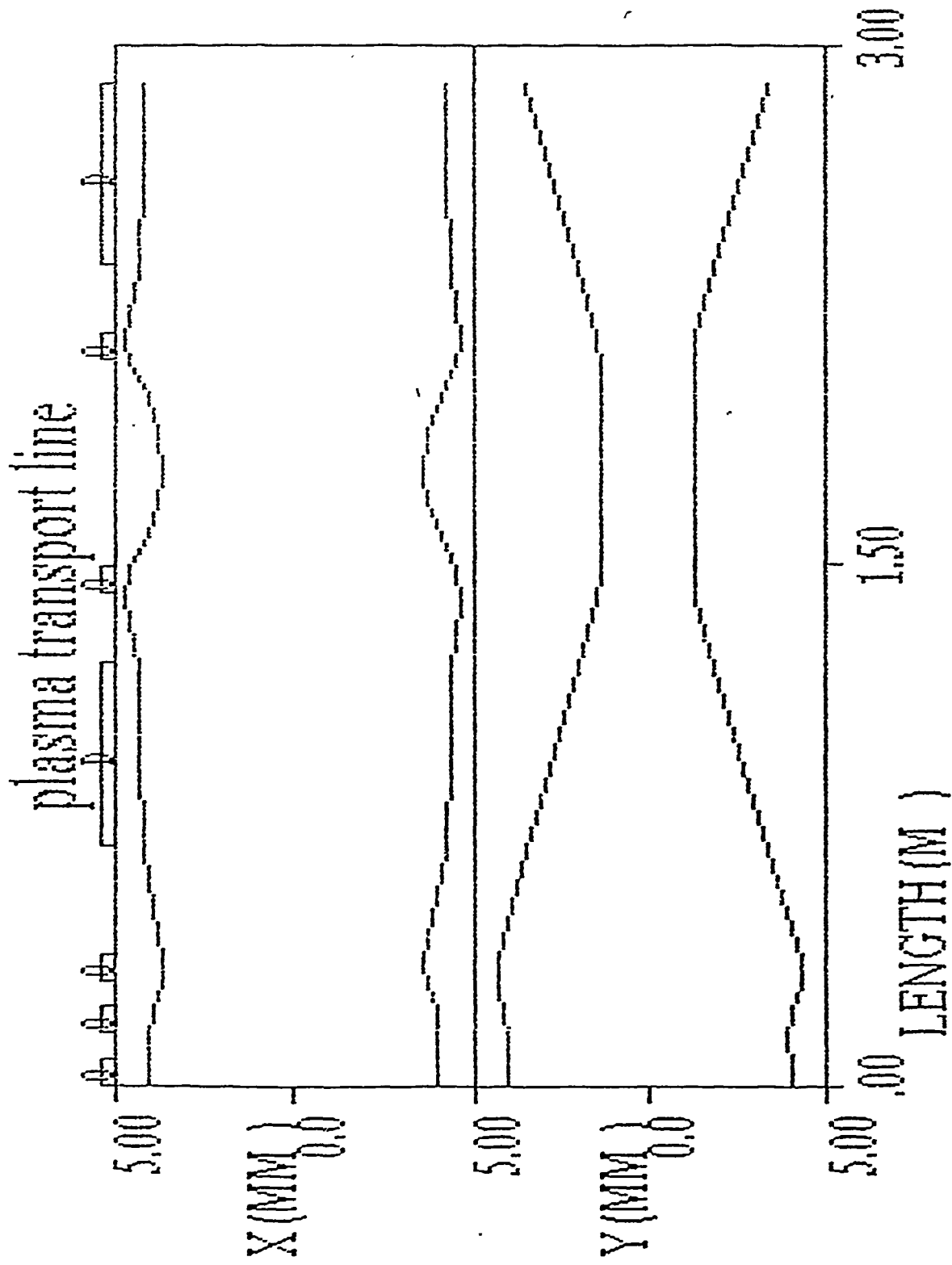
0.3% Energy Spread

plasma transport line NAT1



TRANSPORT Simulation of Beam Line to Plasma

0% Energy Spread



TRANSPORT Simulation of beam Line to Plasma

Correlated Energy Spread $\frac{\Delta E_{head-tail}}{\gamma} = 2\%$

Allows Bunch Compression from 8 ps to $< \sim 1$ ps

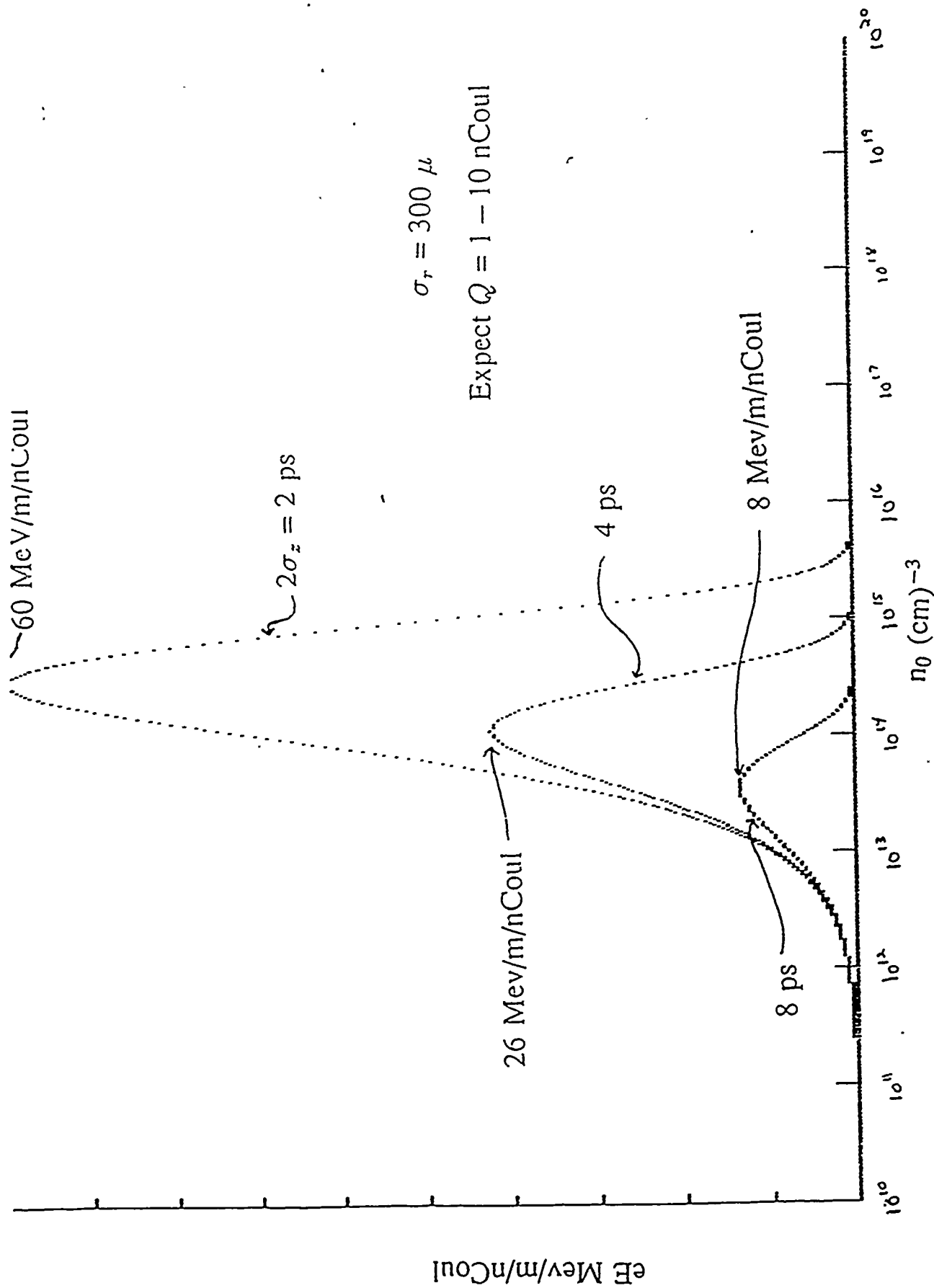
Properties of the PWA Beam Line

The beam line has been designed to achieve three primary goals:

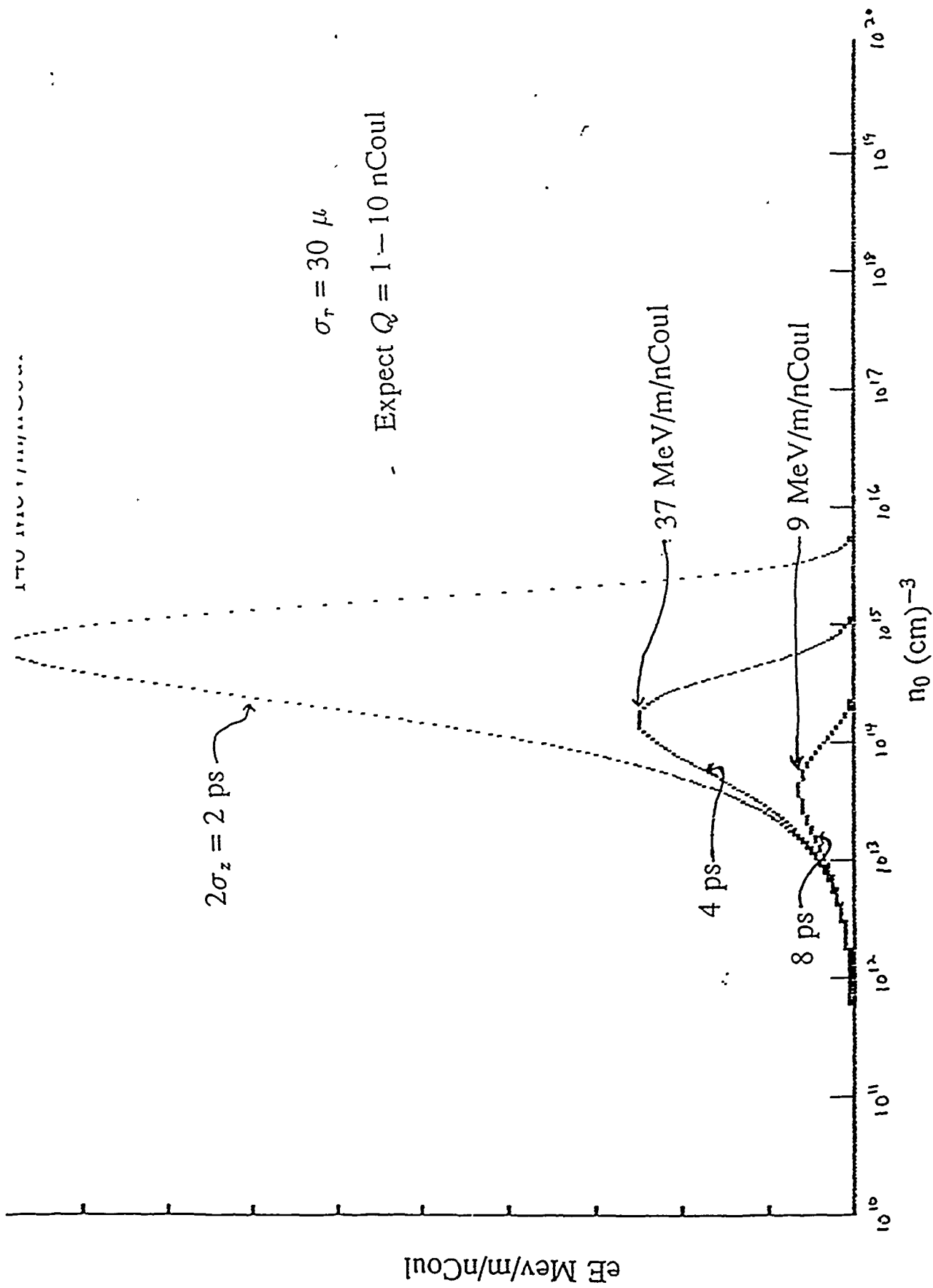
- Directs the beam to the PWA, or allows the beam to go straight to the FEL, providing necessary focusing.
- Has a central focus whose radius is proportional to the energy spread on the beam. This should allow a diagnostic with a resolution of about 0.3% per millimeter.
- Allows for bunch compression option. Pulse can be compressed from 8 ps to ~ 1 ps.

Idea of Bunch Compression

A particle with a higher (or lower) energy than the mean beam energy will follow a longer (or shorter) path through a dipole bending magnet. Thus particles with higher energies will take a longer time to travel through the system. By careful design it is possible to construct a system such that the overall focusing properties of the system are independent of small energy spreads (the system is achromatic) but particles of different energies still follow different trajectories through the system. By using the linac to introduce a linearly correlated energy spread on the pulse, with the leading particles having the highest energy, bunch compression can be achieved. The leading particles follow the longest path lengths, allowing the trailing particles to catch up. The new bunch length is related to the initial bunch length by: $l_{final} = l_{initial} + \frac{\Delta\gamma}{\gamma} R_{56}$. R_{56} for our beam line is -0.1 cm per per cent correlated energy spread.

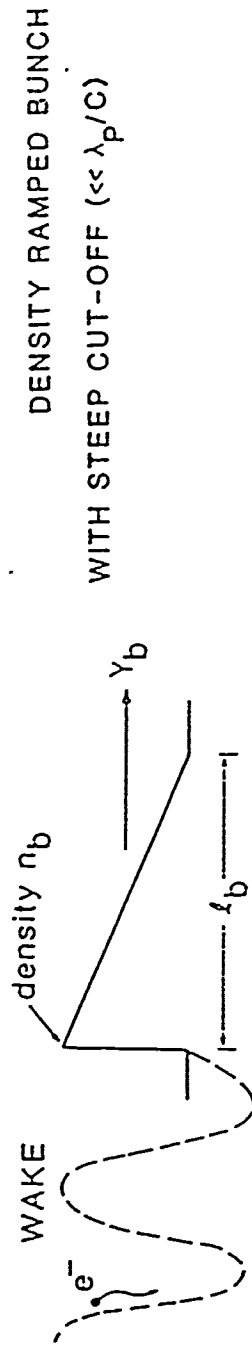


Wakefield Amplitude vs. Plasma Density (Gaussian Beams)



Wakefield Amplitude vs. Plasma Density (Gaussian Beams)

BASICS OF THE PLASMA WAKEFIELD ACCELERATION



- GRADIENT:
$$eE \sim \frac{n_b}{n_0} \sqrt{n_0} \text{ eV/cm}$$
- ENERGY GAIN -TRANSFORMER LIMIT:
$$\frac{E_+}{E_-} = \frac{\Delta\gamma}{\gamma_b} \lesssim R \approx 2nN \equiv \omega_p l_b / c$$
- DEPHASING LIMIT:
$$\Delta\gamma \lesssim 2 \frac{n_b}{n_0} \gamma_b^2$$

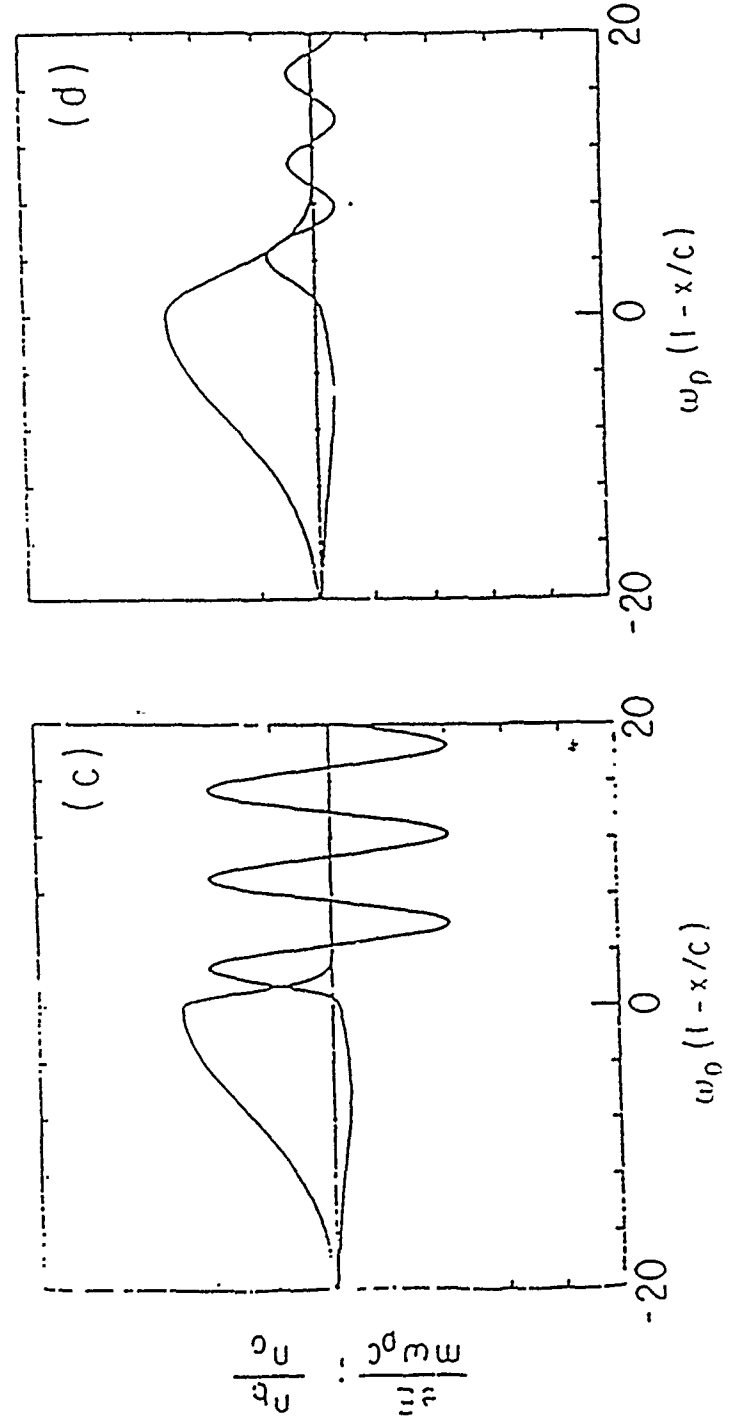
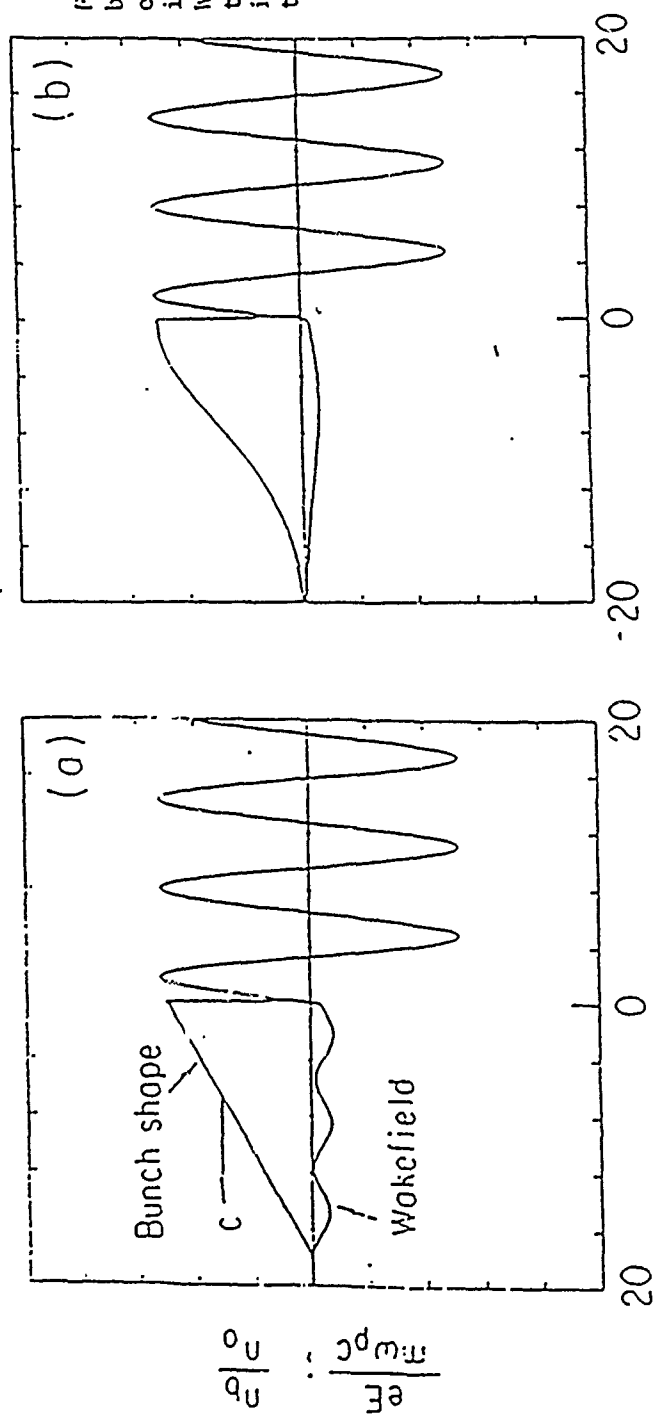


Figure 15 Wake Field Generated by a Shaped Charge Bunch. The electric field inside the bunch is small and decelerating; when the bunch ends abruptly the wake field is large. It ends smoothly, as in (c), the wake field is much smaller.

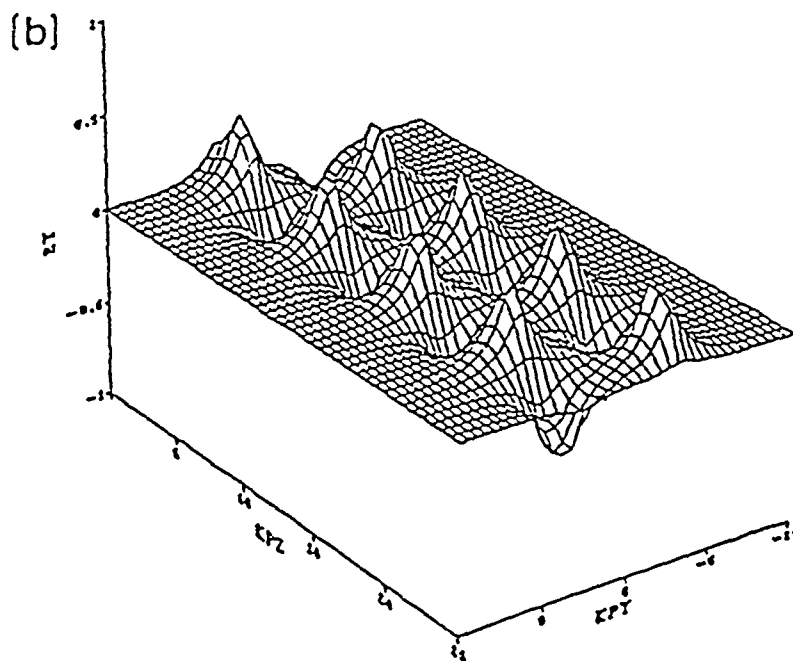
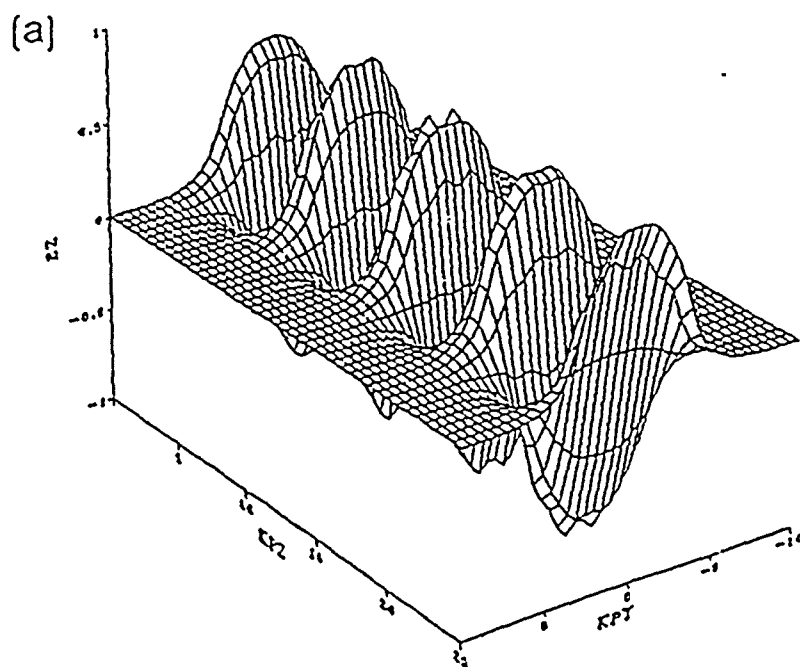


FIG. 2.1. Numerical solution to electron beam generated plasma wave (PWFA). (a) Axial field, and (b) radial field behind a beam beam with a square transverse profile with a diameter of $6 c/\omega_p$.

EXPERIMENTAL, THEORETICAL & COMPUTATIONAL STUDIES OF THE PLASMA WAKE FIELD ACCELERATOR

PROGRESS REPORT NO. 3

October 8, 1990

1. Beam Line Simulations

As discussed in the previous progress report, TRANSPORT simulations showed that bending the beam path prior to the linac section led to unacceptable bunch lengthening and beam degradation. As a result we have re-designed the beam line to separate the FEL and Plasma Wakefield beams after the linac as shown below. Below we summarize the main features of the beam lines.

A. Pulse compression

Originally, we developed a design with two 22.5° bends. This beam line design had all the desired features (see below) except for bunch compression. From TRANSPORT we obtain the R matrix (which operates on the matrix representing the beam envelope in 6-D phase space). This suggests a bunch compression to length

$$l_z = R_{55} l_{z0} + R_{56} \Delta\gamma$$

where l_{z0} is the initial length and $\Delta\gamma$ is the percentage of energy spread on the beam.

For the 22.5° design the R_{56} coefficient was only -.01 suggesting an insignificant compression. By increasing the bending magnets to 45° we found that the R_{56} element didn't just double, but increased eight-fold to -.08. Thus with a 1% correlated energy rise from the front to the back of the beam we can accomplish pulse compression by a factor of 3 (from 4 ps to 1.3 ps).

B. Beam energy and energy spread diagnostic

We have designed the beam line to have a narrow (but chromatic) waist between the quadrupoles labeled Q4 and Q5. The spot size is $100\ \mu$ without energy spread and increases by $\sim 1\text{ mm}$ per 0.1% energy spread. Thus, we should be able to easily measure the beam energy spread to better than $.03\%$ by scanning across the beam spot in $300\ \mu$ intervals.

C. Achromaticity

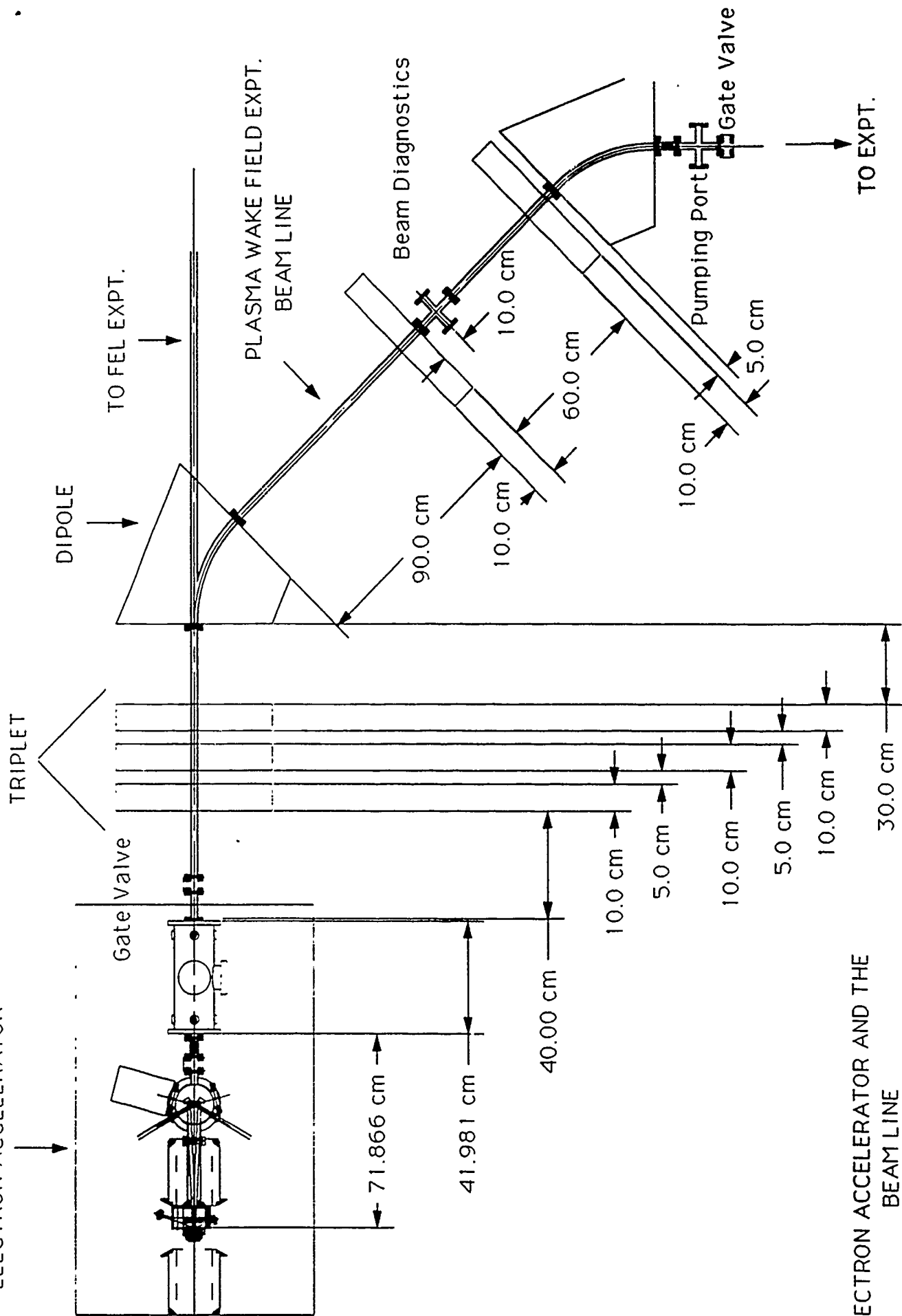
The beam line parameters were fitted to make the beam line achromatic at the end of the second bending magnet (i.e., $R_{16} = R_{26} = 0$). Two bending magnets are the minimum number to satisfy this requirement.

D. FEL Beam Line

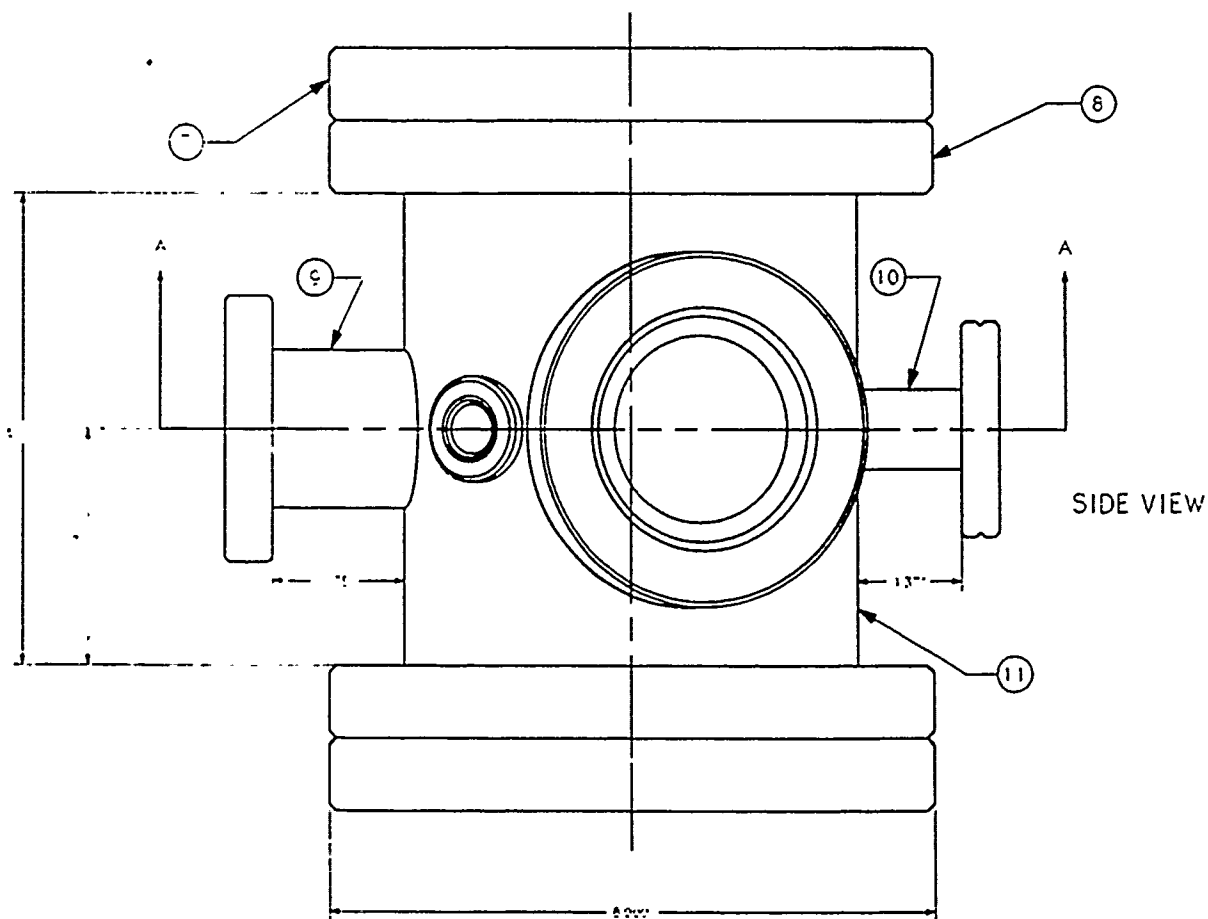
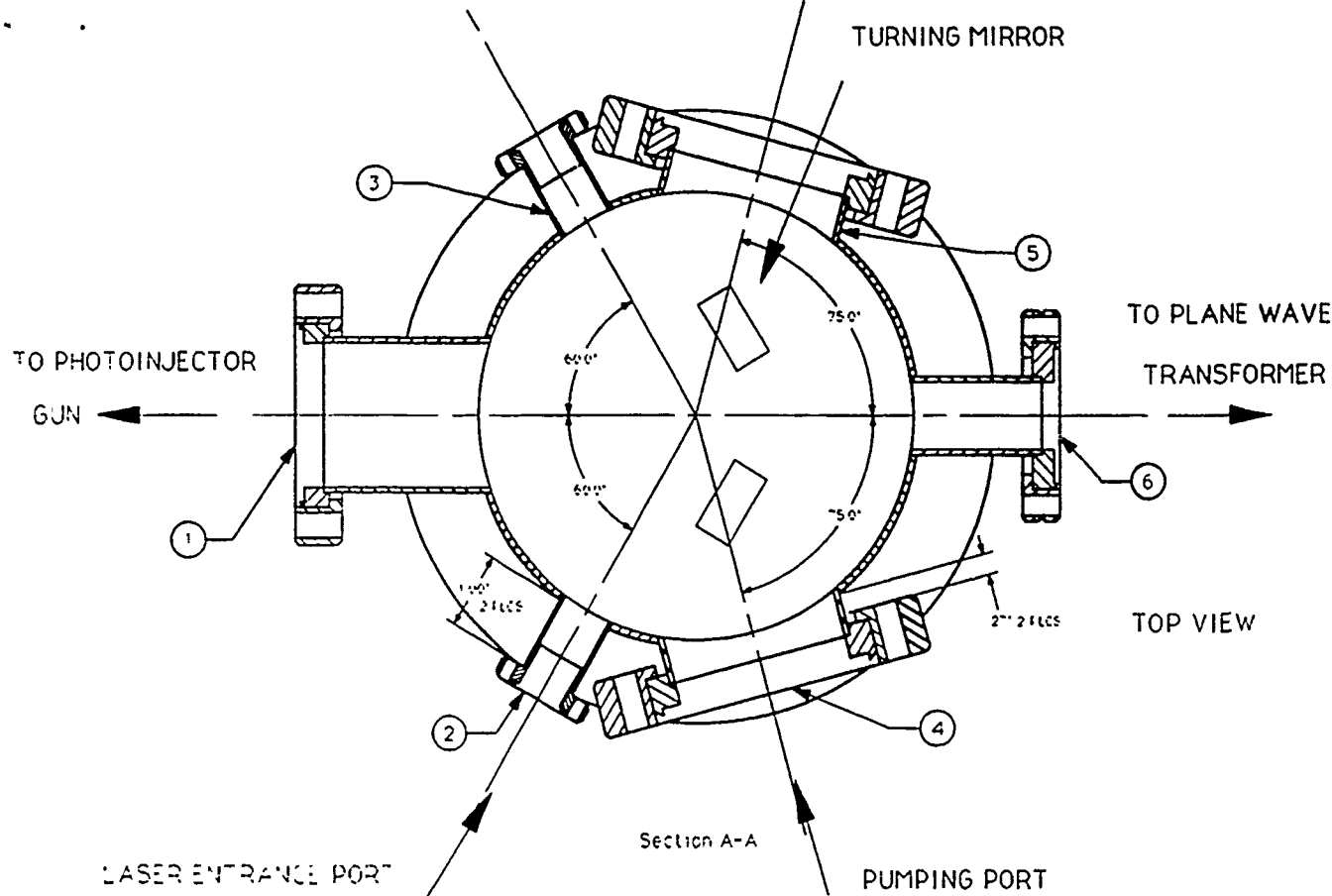
With the first bending magnet turned off, the quadrupole triplet provides a 2 mm waist at the center of the FEL. This spot size was chosen to optimally match to the radiation beam in the FEL.

Parameters and graphical output from the TRANSPORT simulations are attached.

ELECTRON ACCELERATOR

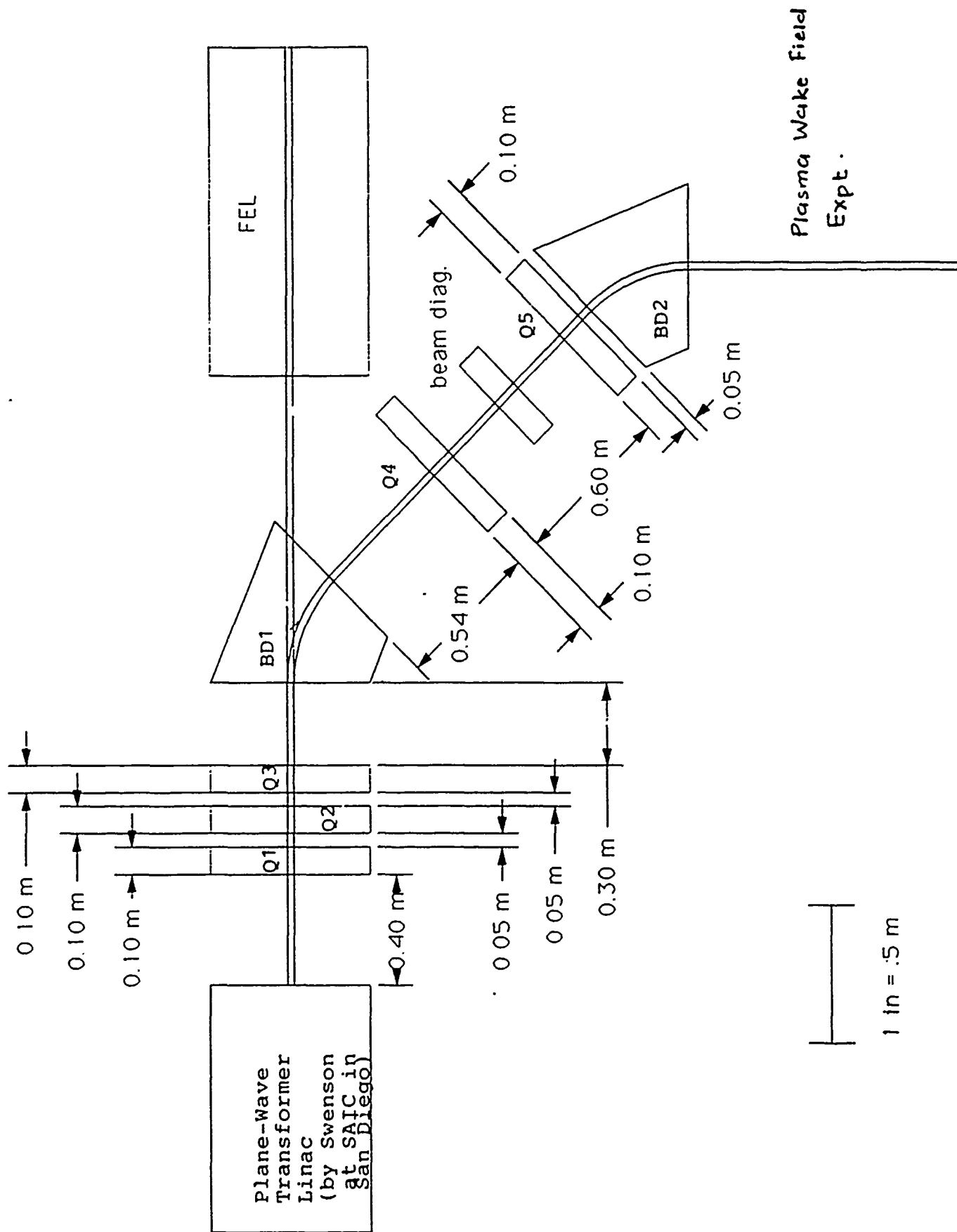


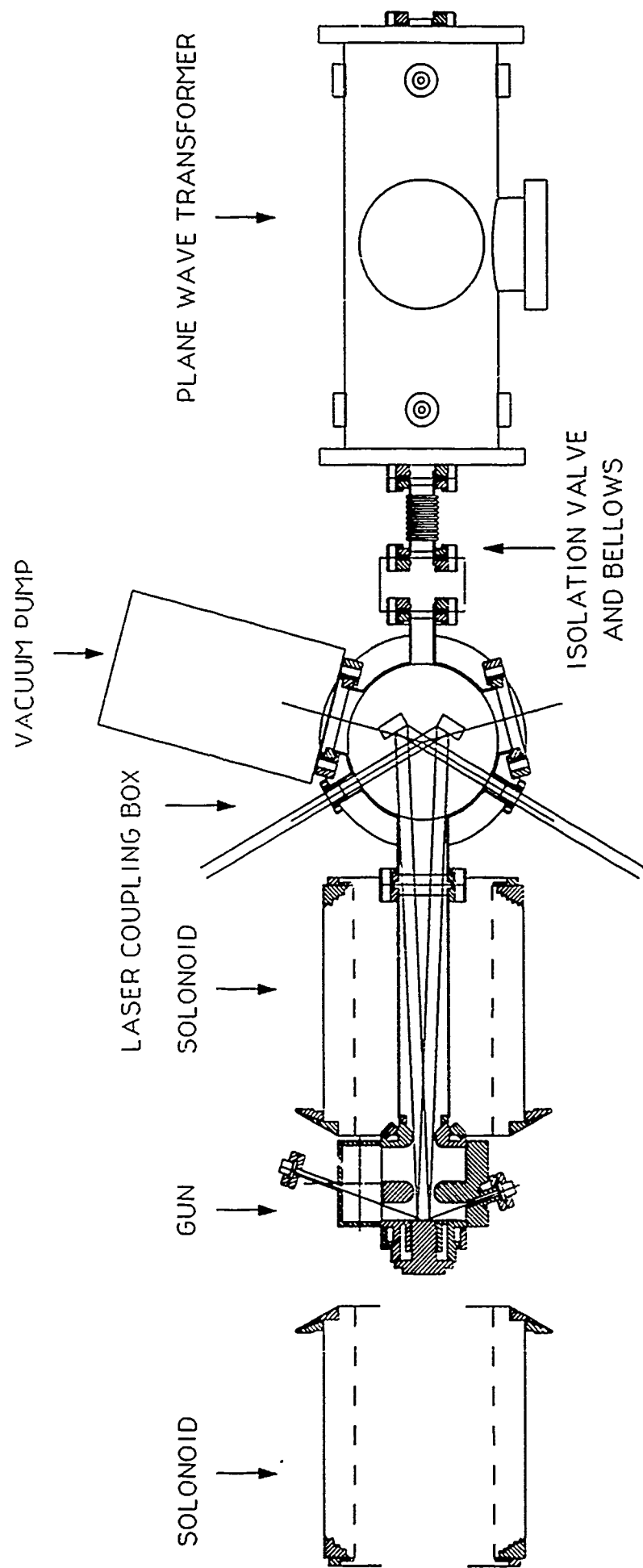
ELECTRON ACCELERATOR AND THE
BEAM LINE



LASER BEAM COUPLING BOX UCLA LINAC

FIGURE 1





THE DETAILS OF THE UCLA PHOTOINJECTOR-DRIVEN ELECTRON LINAC

Figure 3

Laser Coupling Box

The design of a laser coupling box has been completed (fig. 1). This design allows for near normal incidence of the laser beam on the photocathode without interfering with the electron beam. Originally we had planned to bend the electron beam at the exit of the RF gun so that a laser port could be placed normal to the photocathode. Particle transport simulations resulted in a factor of two increase in the electron bunch length. It was decided that a coupling box should be designed for near normal incidence. The important design parameters for the coupling box were:

- 1) The pulse lengthening due to the angle of laser beam incidence must be less than 1ps
- 2) The mirror box must provide an exit port for the laser beam so that electrons are not produced from the reflections of the laser beam within the gun and beam line
- 3) The clearance aperture for the electron beam be greater than or equal to the 2.5 times the RMS diameter of the electron beam.
- 4) The dimensions of the mirror box and the angle of the laser ports must allow clearance for the physical constraints of the system (i.e. the solenoid)

In order to increase the pulse length less than 1ps across a 6 mm photocathode, the laser angle of incidence must be less than 3 degrees. For our design we chose the incident angle to be 2.5 degrees which results in a .87 ps pulse increase. Initially we attempted to use an off axis parabola to focus the beam through a one inch OD beam pipe to the photocathode. This design failed because once the beam reflected off the photocathode it would continue to diverge and therefore irradiate the inside of the gun producing spurious electrons.

To provide an exit port for the laser the beam pipe from the exit of the gun to the coupling box was enlarged to a 2 inch OD beam pipe. This allows room for a 6 mm diameter laser beam to irradiate the photocathode without scraping the beam pipe or RF gun. A symmetric design was used to provide an exit port for the laser beam and also to allow for symmetric radiation of the cathode in the future.

Using "Parmela" the RMS beam radius was determined to be 1 cm at the focus of the solenoid. To provide clearance for the electron beam the required aperture is 2.5 cm. Given this constraint the coupling mirrors were placed 46 cm from the cathode thereby providing a clearance of 2.516 cm for an angle of 2.5 degrees. Due to the proximity of the mirror to the end of the solenoid the laser ports were placed at 60 degrees from the beam axis in order to clear the edge of the solenoid.

DATE: 07/11/1956.

• „Gutachten“ – „Bericht“ – „Entwurf“

work-1: 6 bit value at end of line 2

... the will model the basic line that brings the)

1. *Propaganda* 2. *Propaganda* 3. *Propaganda* 4. *Propaganda* 5. *Propaganda*

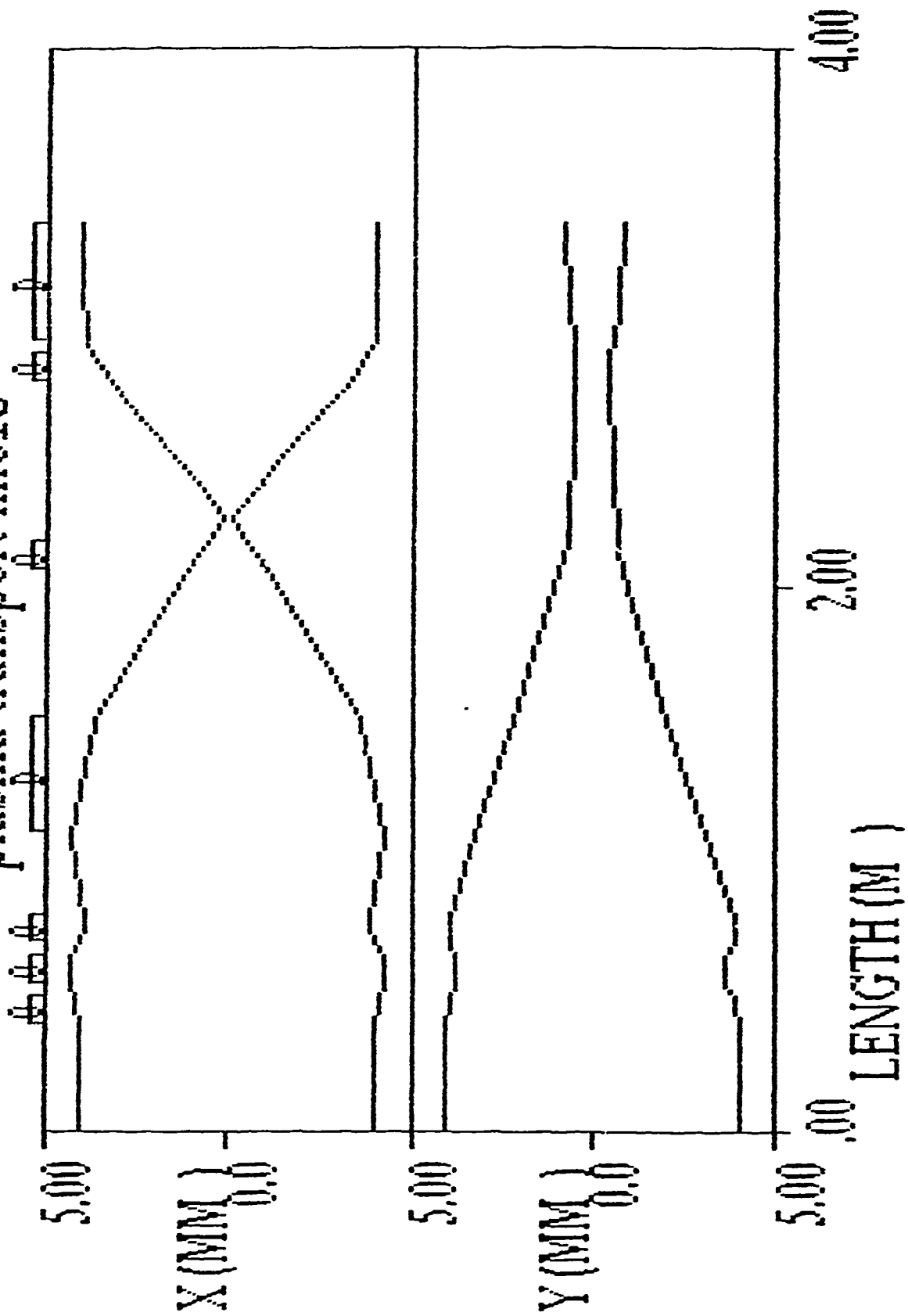
[illegible]

FILED IN DISTRICT COURT OF THE UNITED STATES FOR THE DISTRICT OF COLUMBIA

FORM NO. 10-67 (REV. 1-65) GPO : 1965 O - 345-000-450-2

1. - 2007-06-14 14:00

plasma transport line13



EXPERIMENTAL, THEORETICAL & COMPUTATIONAL STUDIES OF THE PLASMA WAKE FIELD ACCELERATOR

PROGRESS REPORT NO. 2

August 15, 1990

II.1 Laser System

We have now finalized the design of our laser system needed to drive the photoinjector gun. The main components necessary for this system have been ordered. These are: Coherent "Antares" Nd:Yag oscillator and Continuum Nd:silicate regenerative amplifier. The oscillator is a cw mode-locked laser at 38.08 MHz which is the 75th subharmonic of the 2.856 GHz klystron frequency. The crystal oscillator and the Pockel's cell modulator matched to 38.08 MHz have been obtained and sent to Coherent Inc. for incorporation in the oscillator. The table below shows the timetable and what we expect to obtain from the laser system.

		1 μ m	0.25 μ m	When
Coherent: Antares + Continuum regen.	70 ps	15 mJ	2 mJ	Jan 91
Above plus in-house modifications	2 ps(FWHM)	10 mJ	0.25 mJ	March 91

Modifications: In order to generate very short laser pulses we need to employ the "chirped-pulse amplification technique" which has been shown to generate high peak power pulses with extremely short duration. We are currently designing this chirping and compression system and shall report on it in a future report.

Trigger Signal for the Modulator: We shall use a commercial Stanford trigger generator box to fire both the regenerative amplifier and the thyatron which fires the modulator. The output signal will be a standard TTL output.

Optical Table: The laser system will be placed on a 4' x 12' optical table; this has been ordered from Melles Griot.

II.2 Laser Coupling to the Gun

In our last report we discussed why it was desirable to come in as close to normal incidence as possible. At that time we felt that a dipole magnet pair at the exit of the gun would deflect the beam without significant bunch lengthening. Unfortunately, simulations of this "beam-line" using "transport" indicated that at these low energies (4.7 Mev) the bunch easily doubled in length, even when we took care to a) focus the bunch at the input of the first 45% deflection dipole; b) used a solenoidal guiding field to transport the beam between the two dipoles and c) used a second dipole to bring the beam parallel to the original beam path. We discussed this problem with Claudio who suggested that we should try to bring the laser beam either at a shallow angle, or around the electron beam, rather than deflecting the beam. We are currently designing around this possibility.

II.3 Parmela Simulations

Simulations of the electron beam emitted by the RF gun were performed using a modified version of "Parmela" which includes a laser driven photocathode. Using parameters optimized for a 1 nC in 4 ps electron bunch, a simulation of a 10 nC in 4 ps bunch was performed resulting in a temporal lengthening of the bunch from 4 ps to 10 ps. To compensate for this spreading we tried increasing the current in the guiding coil at the exit of the gun from 1700 Amps to 2500 Amps, however, the bunch length increased to 14 ps. By varying the injection phase angle the pulse was shortened to 12 ps at a phase angle of 40°. We then tried increasing the beam radius from 3 mm to 4 mm but no change in bunch length was observed. Since this temporal pulse spreading is unacceptable we will continue running simulations beginning with 1 nC in 40 ps (which showed no pulse spread) and gradually increasing the charge while decreasing the pulse length. We will optimize the injection phase and coil current to minimize the pulse length for each increment.

II.4 Beam Line Simulations

TRANSPORT was used to model beam transport from the gun to the plasma experiment. A summary of the conclusions is given below:

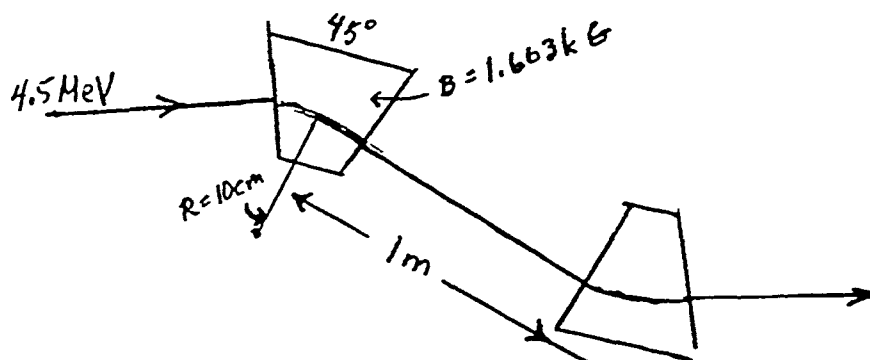


Fig. 1 4.5 MeV Beam line schematic

- a) With two 45° dipole bending magnets only--the beam blows up in the 1 m drift space and bunch lengthens from 1 ps (half-width) to 10 ps
- b) With solenoidal focusing between the magnets and after--emittance remains below 60π mm-rad; bunch lengthens from 1 ps to 3 ps; matched solenoidal field (B_z chosen such that $v_\perp/\Omega_c = \sigma_x \approx 5$ mm) of 1.92 kG is optimal.

To overcome the bunch lengthening a new beam line system was suggested by C. Pellegrini. Two 22° bending magnets are used after the linac section when the beam is at 20 MeV rather than 4.5 MeV. These will serve both as a switchout between the plasma wakefield/FEL experiment and as a beam energy and energy spread diagnostic (see Fig. 2) TRANSPORT will be used to optimize the beam line parameter.

II.5 Optimizing Wake Field Accelerator Experiments

We decided to postpone any further work on the wake field acceleration simulations until we have a better idea of the realistic electron beam parameters through PARMELA and TRANSPORT simulations.

II.6 Personnel Update

We have hired a postdoctoral researcher, Dr. Garnick Hairapetian, who obtained his Ph.D. from Prof. R. Stenzel's group to work on the Plasma Wake Field Accelerator project. Garnick's main responsibility will be to work on the design, construction and diagnostics of the plasma source as well as on the diagnostics for the acceleration experiment.

II. 7 Pulse Shaping Option

Although the primary plan for laser injection is at near normal incidence (see previous report), the gun has ports which allow laser incidence at 70° . It was realized that this can be used to produce shaped electron bunches of the type needed for a high transformer ratio wakefield experiment as follows.

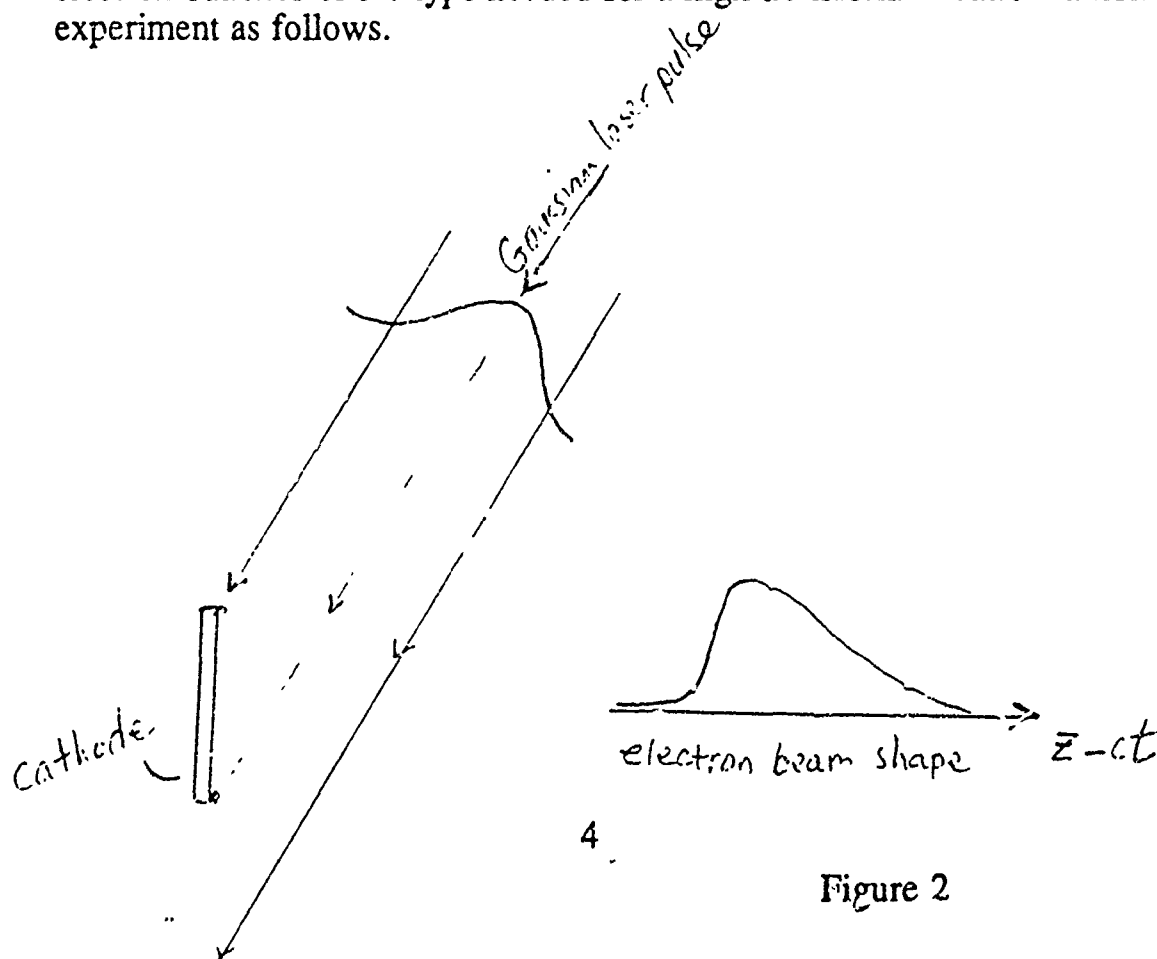
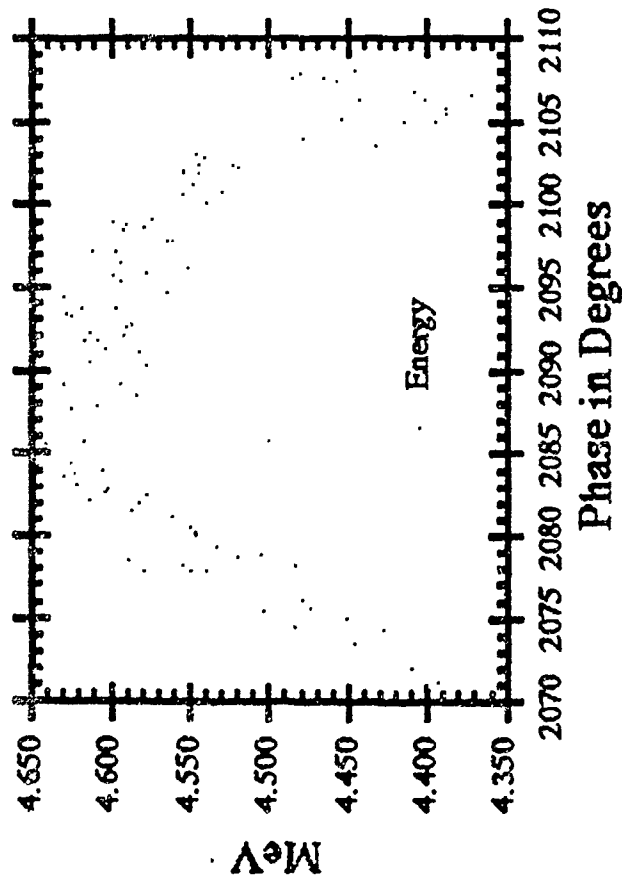


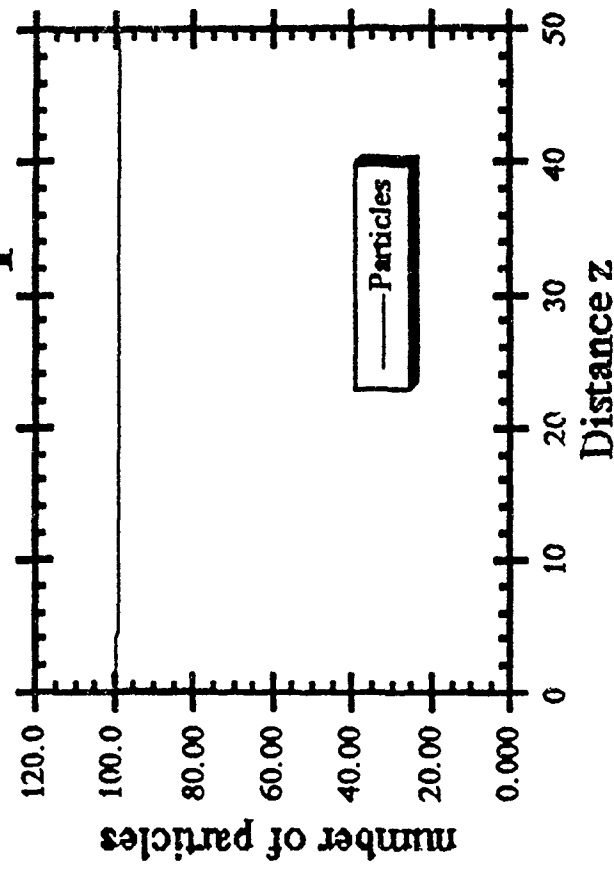
Figure 2

The center of the laser hits the lower portion of the cathode later than does the outer (left) portion of the laser due to its added path length as shown in Fig. 2. Since the center is more intense, more electrons are liberated by it giving rise to the temporal shape shown.

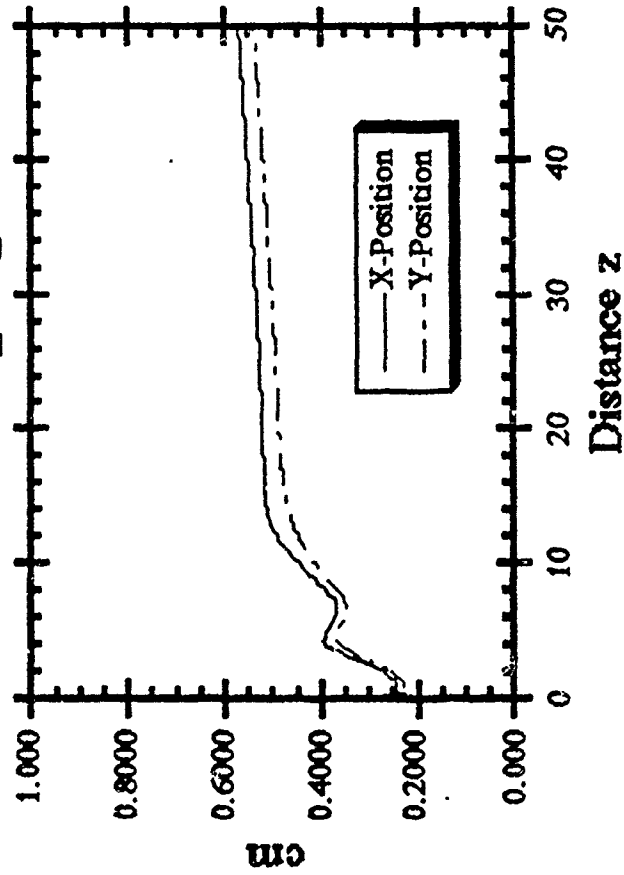
10ncx40psxengyph-good



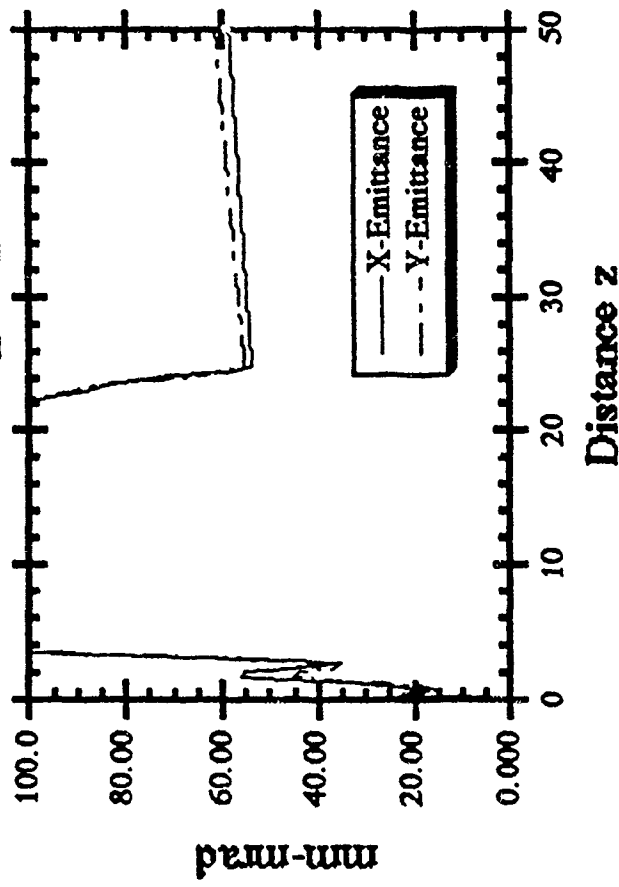
10nC 40ps



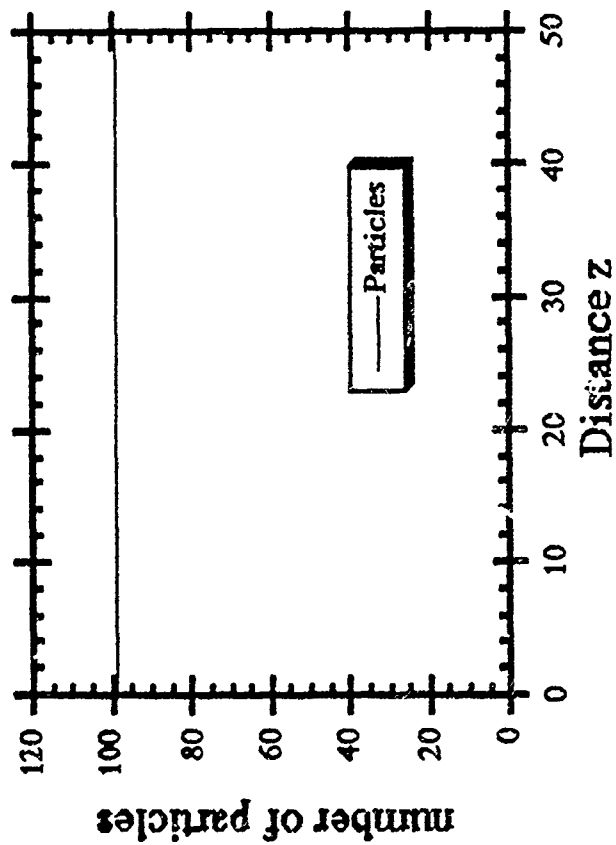
10ncx40ps-good



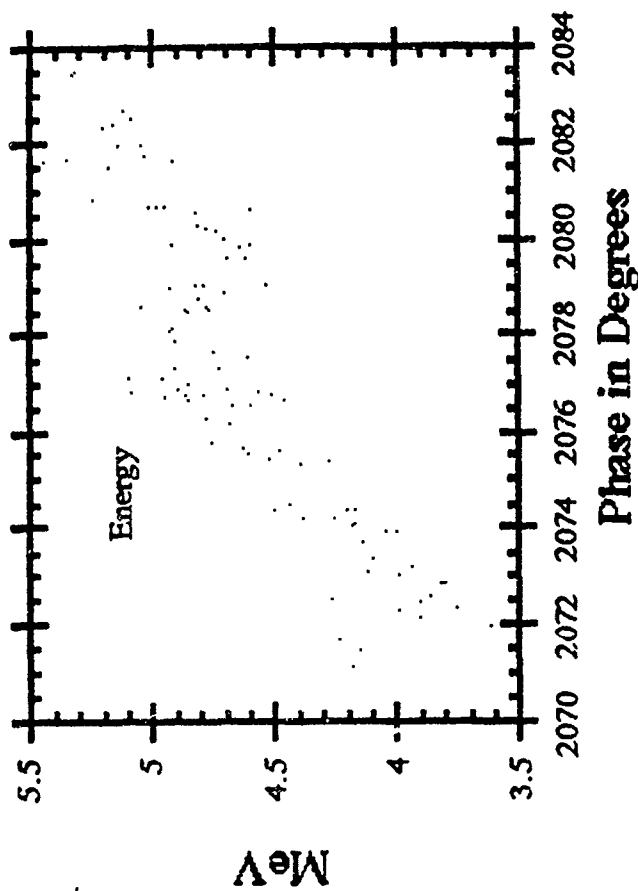
10ncx40ps-good



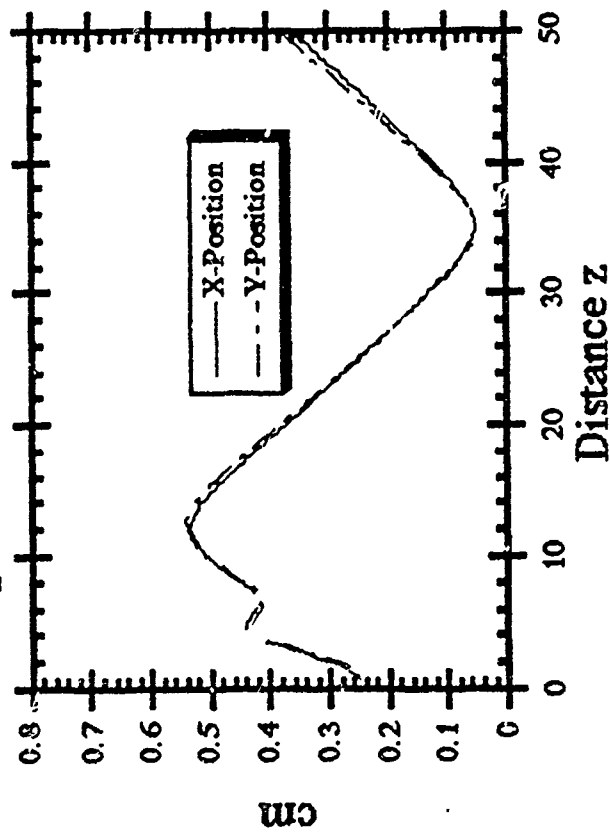
4psx3x2500x55.testmac



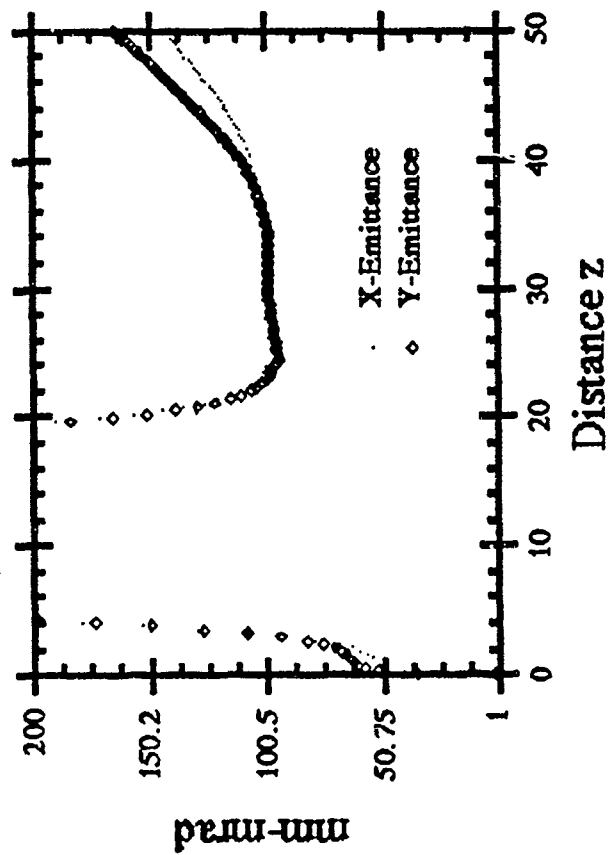
4x3x2500x55.testmac



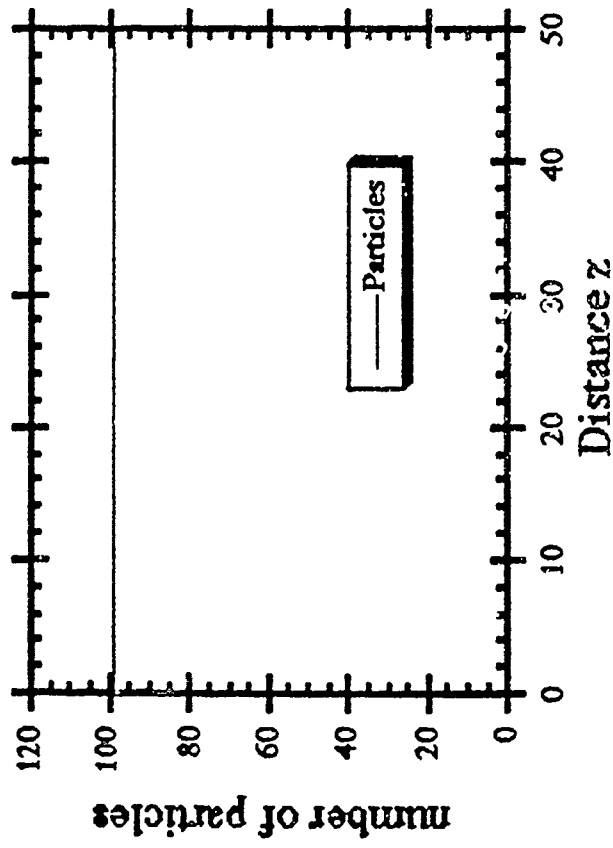
4psx3x2500x55.testmac



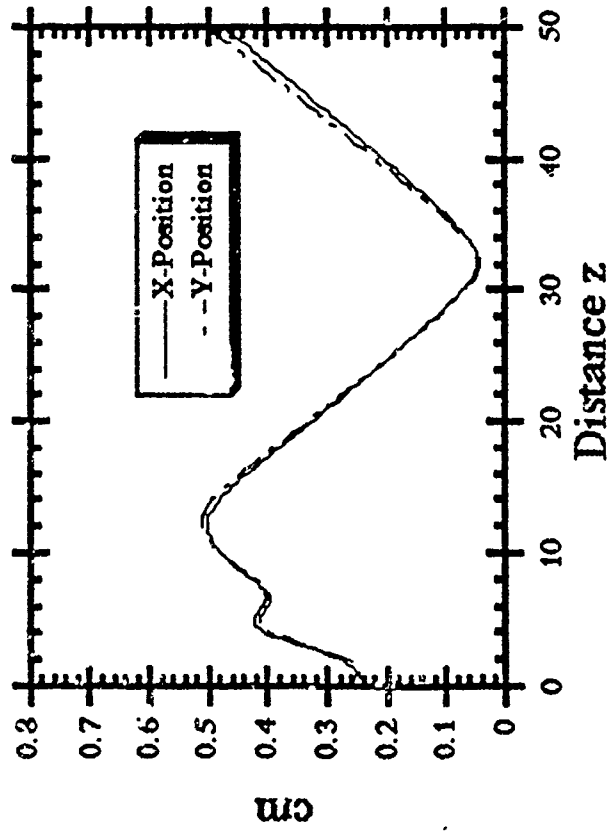
4psx3x2500x55.testmac



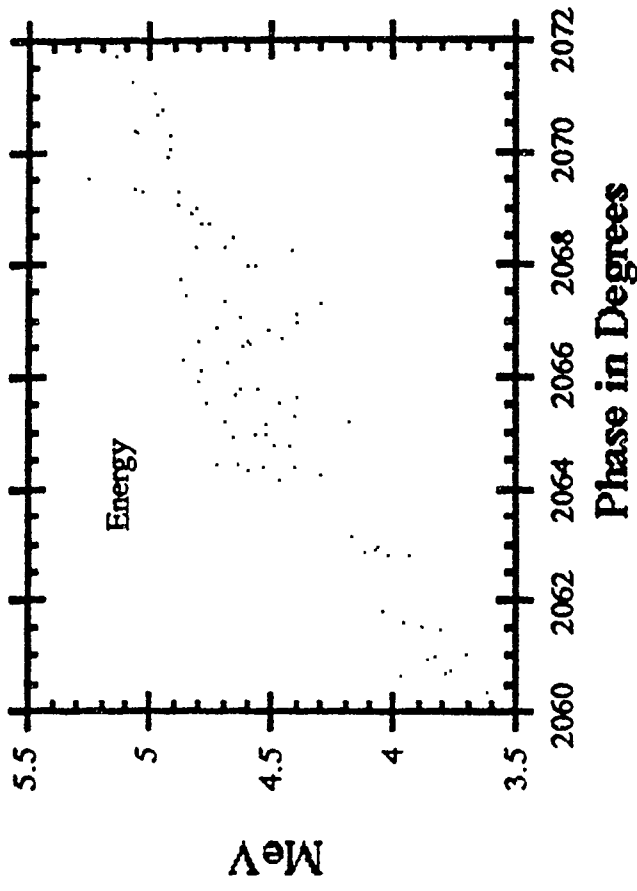
4ps3mm2500amp40.mac



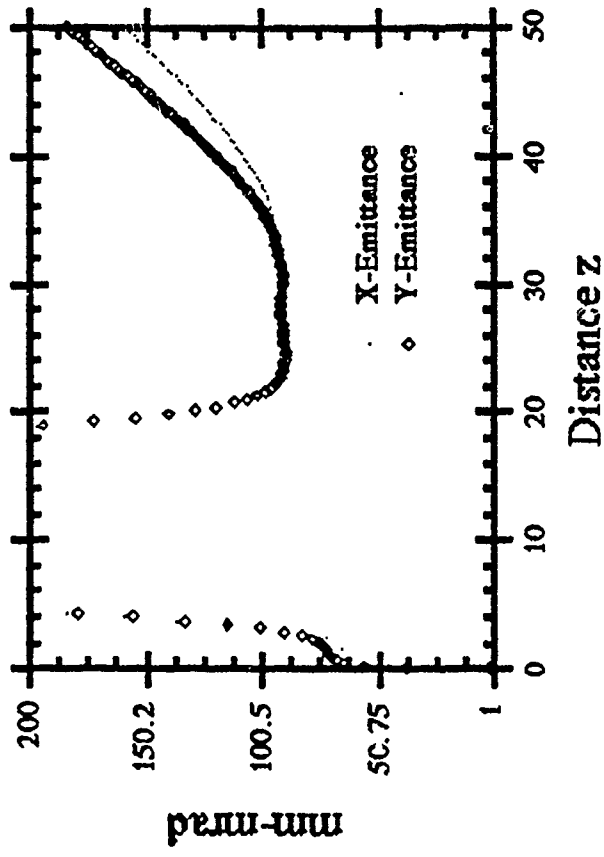
4ps3mm2500amp40.mac



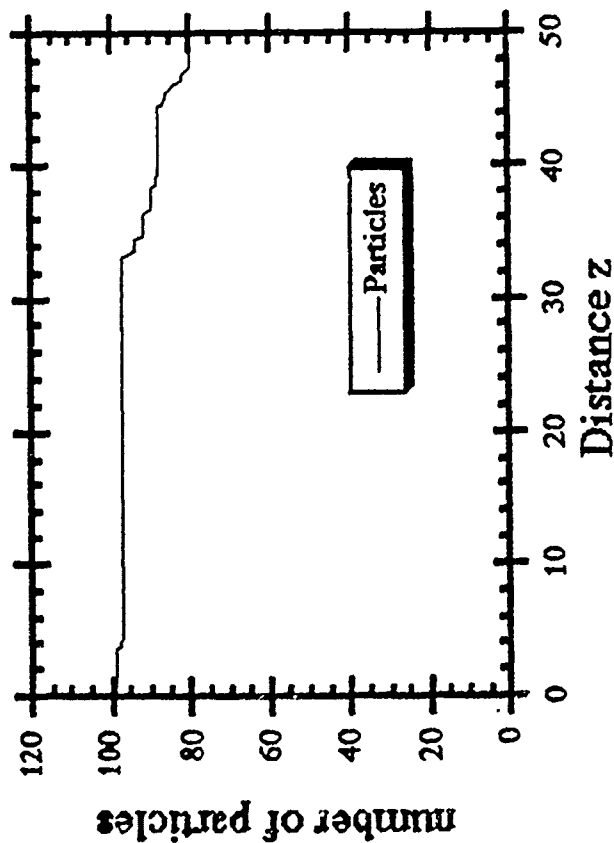
4psx3x2500x40.mac



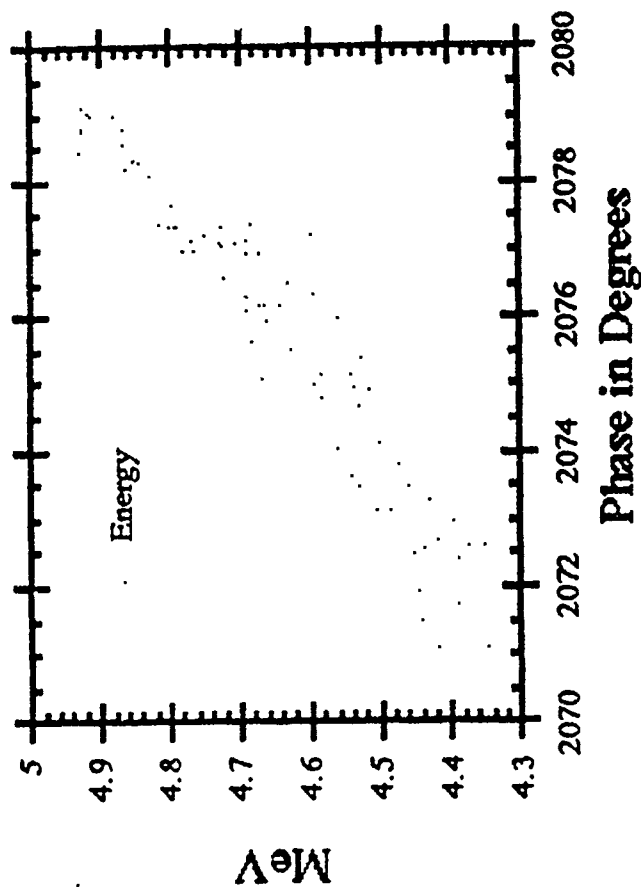
4ps3mm2500amp40.mac



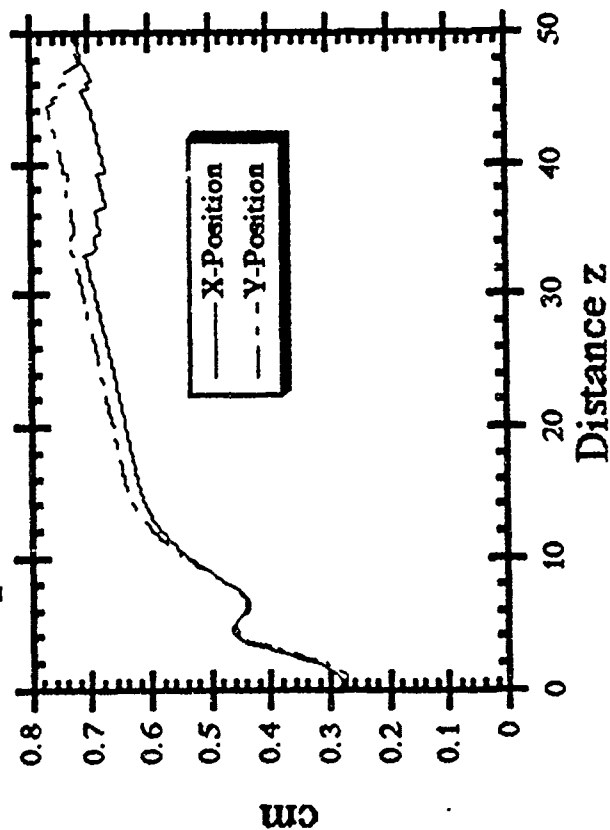
4ps4mm1700amp55.mac



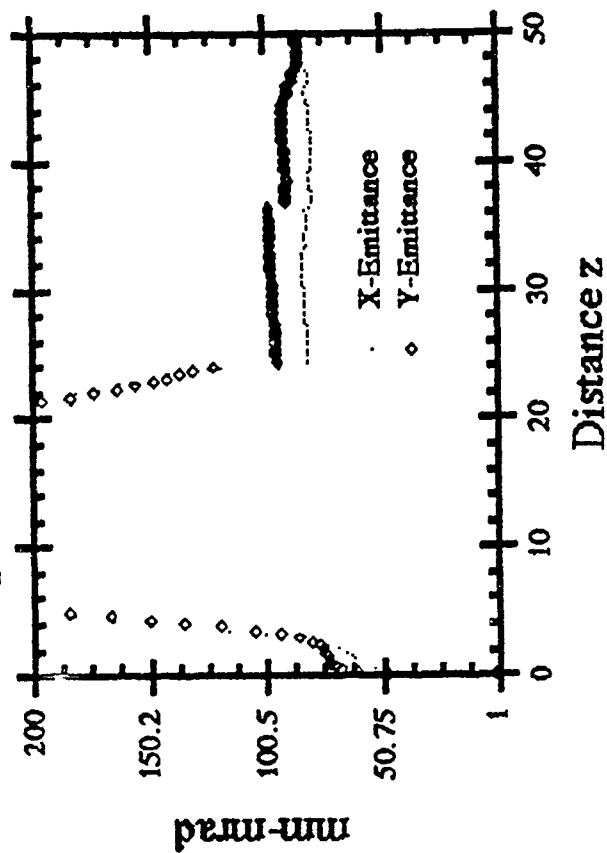
4psx4x1700x55.mac



4ps4mm1700amp55.mac



4ps4mm1700amp55.mac



**EXPERIMENTAL, THEORETICAL & COMPUTATIONAL STUDIES
OF THE PLASMA WAKEFIELD ACCELERATOR
PROGRESS REPORT #1**

July 15, 1990

I. Introduction

A core group comprised of Professor C. Joshi, T. Katsouleas and students P. Davis and J. Smolin meets weekly to coordinate theoretical/experimental efforts on the wakefield experiment. This is a summary of progress made since the first meeting in 6/26/90.

II. Photocathode Injector Geometry

It was recognized immediately that the original photocathode-gun design would not be suitable for producing short electron pulses. This is because the original plan was to illuminate the cathode at a glancing 70° angle w.r.t. the normal. The time difference between arrival of the laser at the top and bottom of the cathode gives greater than at the picosecond pulse spread. We explored the use of a diffraction grating to compensate the paths of different rays, but dispersion from the laser bandwidth still leads to a picosecond pulse broadening out to about 4 ps. It was decided to explore the possibility of normal incident illumination of the photocathode using laser light as shown in the figure 1. A mach-zehnder set up was suggested for producing two laser pulses with roughly 80:1 intensity ratio and a variable delay between the pulses. We shall talk to Claudio about these changes. A single dipole magnet after the gun will probably suffice to deflect the beam either towards the diagnostics beam line or towards the main beam line. These two beam lines will be orthogonal to one another and at 45° to the laser entrance port.

III. Laser Design

We shall order the Coherent Antares oscillator and Continuum - Nd:(silicate) glass regenerative amplifier in the next one month. The CPA technique will be used to generate pulses of about 2 ps duration (FWHM) containing > 10 mJ of energy at $1\text{ }\mu\text{m}$. In the first instance we will get about $1/2$ mJ of energy at $0.25\text{ }\mu\text{m}$ to drive the photocathode at 1 Hz. This can later be upgraded to 5 Hz and 1 mJ. The tentative plan is as follows.

	Deadline
Order lasers	Aug.1, 1990
Order optical tables, optics, etc.	Aug. 15, 1990
Laser operational at 50 ps level	Jan. 30, 1991
Laser operational at 2 ps level	June 1, 1991
Laser improvement and upgrade	beyond June 1991

IV. Upgrade of Beam Charge

The original photocathode design from BNL is for a 1 nC charge bunch. For our experiment we need to upgrade this to 10 nC. We will do this through a combination of higher laser energy and higher quantum efficiency cathode material (LaB_6 at $\text{QE} > 10^{-5}$). We estimate that a 1 mJ laser will exceed by a factor of 10 the number of photons needed.

We also estimated the space charge limits of the 10 nC bunch. The bunch's space charge field is 7 MV/m, still well below the applied 100 MV/m of the RF. To verify that space charge is not a problem we performed PARMELA simulations (attached) of a 10 nC, 4 ps pulse. The results show that more than 80% of the beam makes it through the 50 cm injector with an emittance of 8 mm-mrad and spot size of 6 mm. However, pulse lengthening to 8 psec is observed, and the causes need to be identified. The pulse lengthening may be avoidable by optimizing the solenoid strength at the output of the gun.

V. Optimization of Plasma Parameter

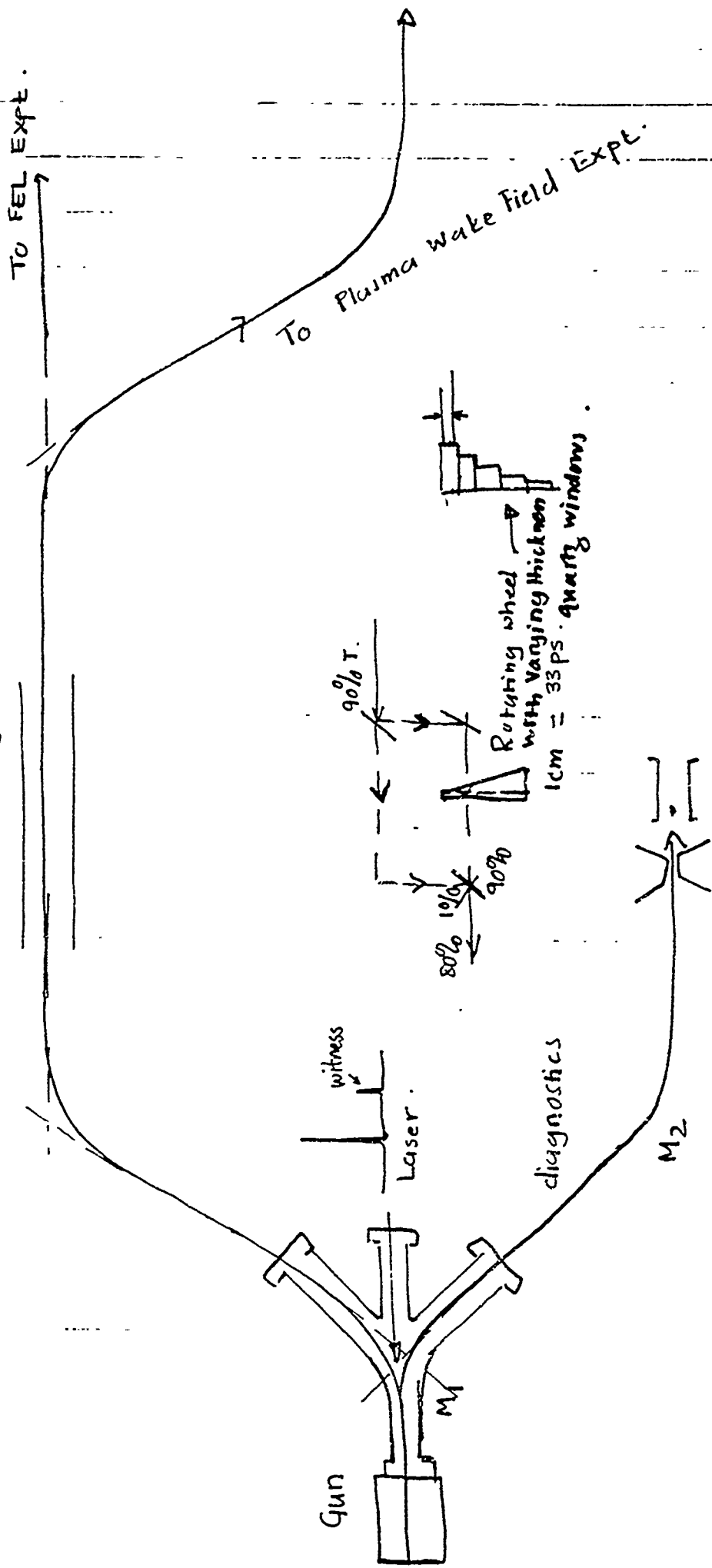
Linear plasma wakefield theory was applied to our expected beam parameters. Numerical solutions showing accelerating gradient vs. plasma density are shown below for various bunch lengths and radii. These show that the optimal plasma density is near $1 \times 10^{14} \text{ cm}^{-3}$. Further modeling of beam self-pinching using a 2D PIC code is planned.

VI. Manpower

We need to add an experimentalist to our team. We have several very good applicants and hope to recruit a suitable candidate within the next couple of months.

7-10-90

Accelerating Structure .



Pump .

- Magnets M₁ and M₂ .

- Beam line .

Fig 1 .

Sketch of the gun, the beam line and the accelerating structure

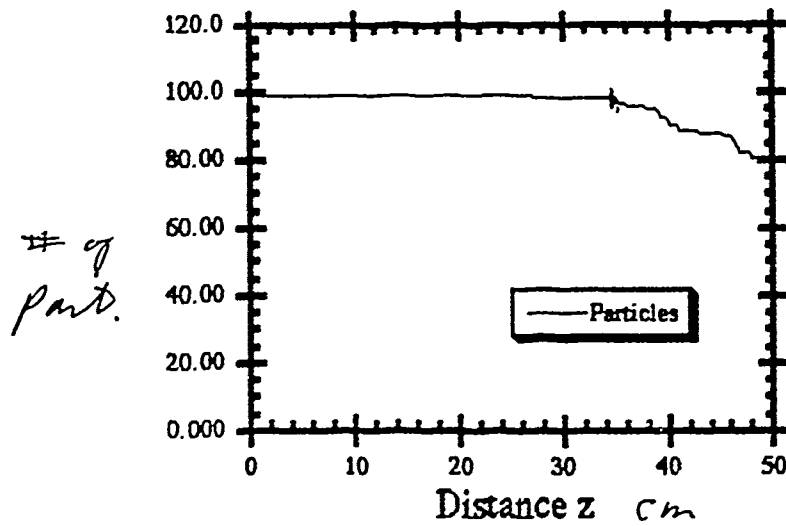
.8C , PAMELA INPUT FOR UCLA RF GUN

```
run 1 1 2856. 0. 1.0e-6 1
output 0 0 1 0 0 0 1
input 0 99 2000 2.0 .3 .6 1.0e-6 3.e-8 0.5
cell 2.625 1.0 0 0. 100.0 1. 10. -1. 0. 0. 0.
cell 2.625 1.0 0 180. 100.0 1. 10. 1. 0. 0. 0.
cell 2.625 1.0 1 180. 100.0 1. 10. -1. 0. 0. 0. 30 1
0.1024080e+01, -.1231721e-01, -.1447282e-01, 0.3216015e-02, -.5719878e-03,
0.7671146e-04, -.1198880e-04, 0.1151588e-05, -.2941766e-06, 0.3205865e-07,
-.2252848e-07, 0.3576355e-08, -.2063014e-08, 0.2789092e-09, -.1618336e-09,
0.1734898e-10, -.1253869e-10, 0.8872545e-12, -.9003462e-12, -.3870712e-13,
-.3449617e-13, -.2450825e-13, 0.4857463e-14, -.5318912e-14, 0.1490762e-14,
-.8461214e-15, 0.2428480e-15, -.1070874e-15, 0.3108925e-16, -.1996790e-16,
coil -9.375 2.0 -1700.0 -1. 24.00
coil -9.375 4.0 -1700.0
coil -10.375 2.0 -1700.0
coil -10.375 4.0 -1700.0 - Amps
coil -11.375 2.0 -1700.0
coil -11.375 4.0 -1700.0
coil -12.375 2.0 -1700.0
coil -12.375 4.0 -1700.0
coil -13.375 2.0 -1700.0
coil -13.375 4.0 -1700.0
coil -14.375 2.0 -1700.0
coil -14.375 4.0 -1700.0
coil 9.375 2.0 1700.0
coil 9.375 4.0 1700.0
coil 10.375 2.0 1700.0
coil 10.375 4.0 1700.0
coil 11.375 2.0 1700.0
coil 11.375 4.0 1700.0
coil 12.375 2.0 1700.0
coil 12.375 4.0 1700.0
coil 13.375 2.0 1700.0
coil 13.375 4.0 1700.0
coil 14.375 2.0 1700.0
coil 14.375 4.0 1700.0
drift 16.0 1.5 0
drift 34.0 1.5 0
scheff -6.e10 1.0 .3 10 18 0 0. 0 1.5 0. -1.75
start 55. 0.1 250000 1 100
save
zout
end
coil 7.375 5.0 9000 7.275 7.475 -1 18
cell 2.625 1.0 0 0. 100.0 1. 10. 1. 0. 0. 0.
cell 2.625 1.0 0 0. 100.0 1. 10. -1. 0. 0. 0.
cell 2.625 1.0 0 180. 100.0 1. 10. 1. 0. 0. 0.
cell 2.625 1.0 1 180. 100.0 1. 10. -1. 0. 0. 0. 30 1
```

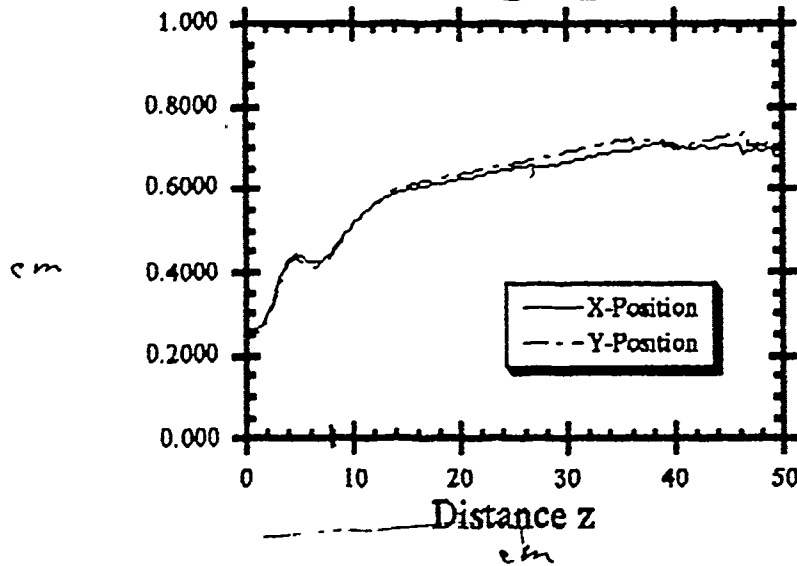
VI Manpower.

We need to add an experimentalist to our team. We have several very good applicants and hope to recruit a suitable candidate within the next couple of months.

10ncx2ps.good

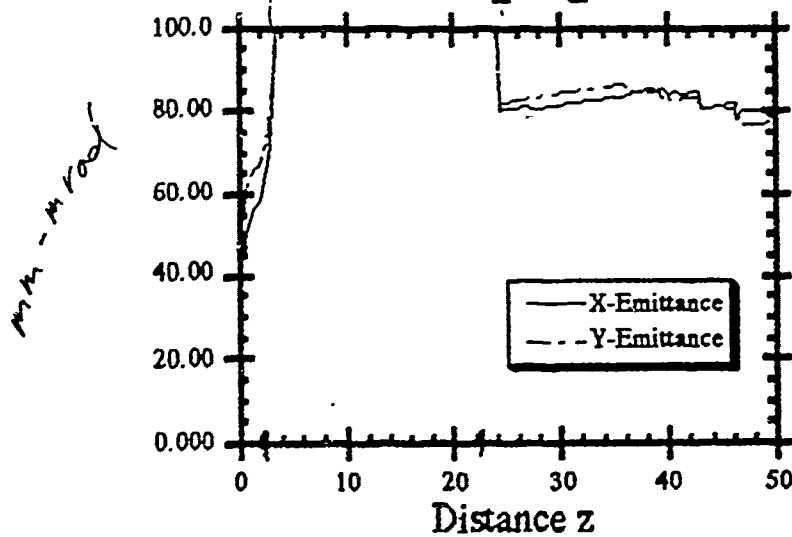


10ncx2ps.good



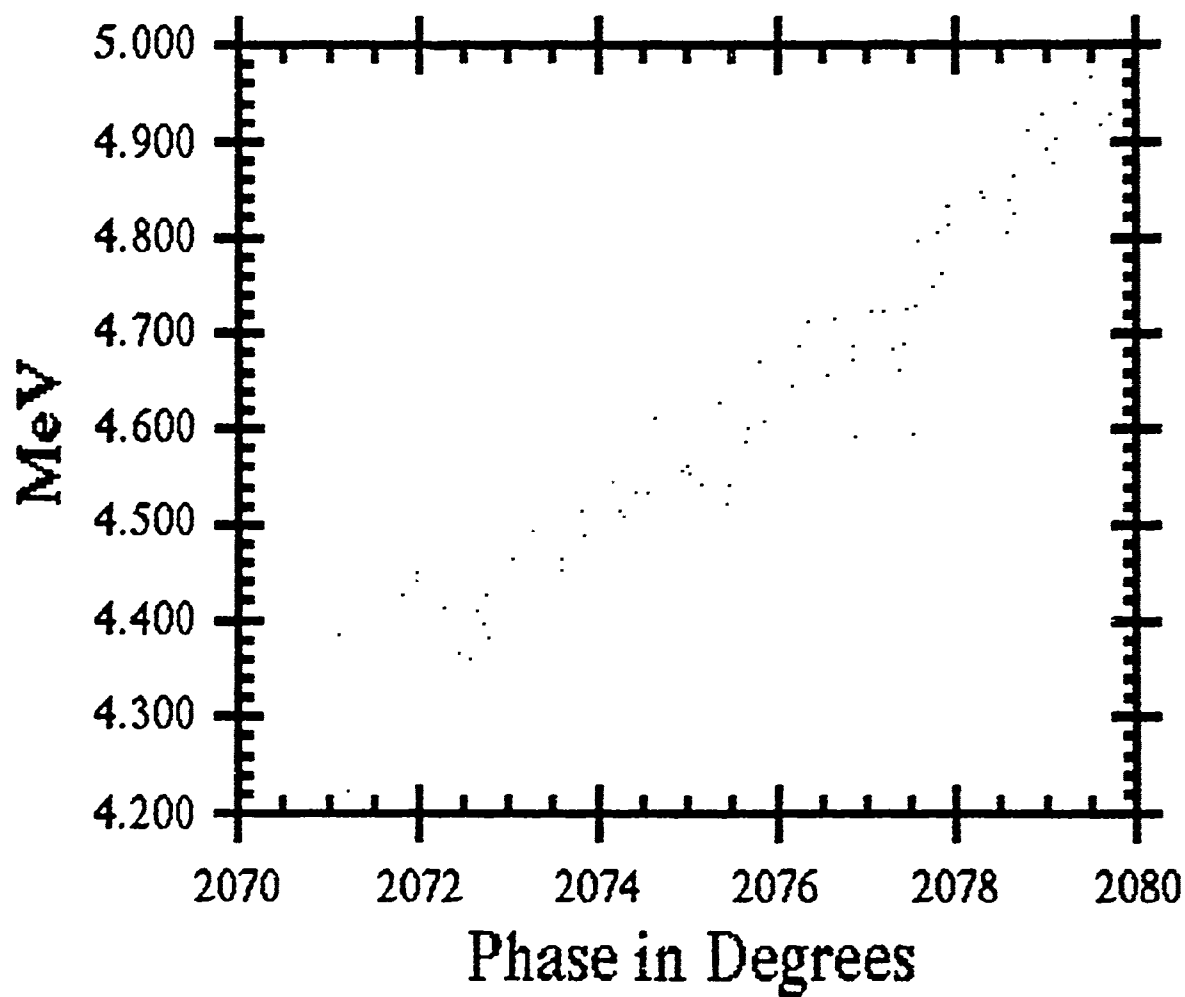
RMS

10ncx2ps.good



RMS

10ncx2psxengyph.good



$1^\circ \sim 1\text{ps}$
 18°
 width $\sim 8\text{ps}$ (initially 4ps)
 \Rightarrow need coil redesign